Pipe Flow Modeling for Ultrasonic Flow Measurement Instrumentation

U.S. Export Control

LICENSED MATERIAL

WARNING:
Please read the Export Control and License Agreement on the back cover before removing the Wrapping Material.

Technical Report

EPRI *Powering Progress*

R E P O R T   S U M M A R Y

Pipe Flow Modeling for Ultrasonic Flow Measurement Instrumentation

This report considers potential improvements in the instrumentation developed for ultrasonic flow measurement of the primary coolant in a pressurized-water reactor. A computer-based model was developed to estimate the flow profile correction factor for non-ideal flow conditions, which is typical of that encountered on hot-leg piping where such instrumentation is installed. Currently, the correction factor is determined for nominal conditions descriptive of the piping configuration. The model considers variations of the profile factor for two configurations: the Contraction Model to simulate a reducer section and the Spherical Model to simulate flow conditions exiting the steam generator. The modeling was conducted using a three-dimensional finite element computer model developed by the contractor.

INTEREST CATEGORIES

Instrumentation and control
Assessment and optimization
Licensing and safety assessment
Plant thermal performance

KEYWORDS

Instrumentation and control
Primary coolant
Plant thermal performance
Ultrasonics equipment
Calorimetry
Modeling
Flow measurement

Background Ultrasonic instrumentation to measure primary coolant mass flow utilize a flow profile correction factor to the computed velocity to estimate the diametral velocity. This correction factor is dependent on several conditions related to the ultrasonic flow meter configuration; piping geometry, flow conditions, coolant pressure, and temperature. Using a nominal correction factor, estimated for laminar flow and assumed process conditions, could lead to significant errors. Computation of the profile factor requires performing an accurate and mathematically intensive finite-element analysis with adequate resolution to accurately compute the parameters at each node. EdF has developed a code implemented on a fast supercomputer, along with other simulation software that can configure and analyze the piping geometry of interest.

Objectives

- To develop flow models for specific piping configurations for which experimental results were available
- To modify existing models to simulate ultrasonic flow measurement capabilities
- To calculate flow profile factors for varying ultrasonic entry angles, axial positions, and fluid flow conditions
- To perform parameter sensitivity analysis to determine important plant-specific conditions that must be modeled

Approach The project team identified piping configurations of importance to determine the flow profile correction factors to be used for an ultrasonic flow measurement system. Experimental data were previously obtained in a separate project in order to validate the modeling results. The team simulated the ultrasonic instrumentation in order to model the variation in ultrasonic parameters (for example, beam angle, transducer position, etc.) on flow profile correction factors. Two piping models were analyzed: the Contraction Model to simulate the effect of a 24"-to-16" reducer connected to a 40° elbow and then to a straight piping run; and a Spherical Head Model to simulate the piping configuration at the bottom of a steam generator.

Results The profile factors obtained with the tool are overall in good agreement with the experimental data. For the Contraction Model, the typical difference between experimental and numerical profile factors is less than 3%; however, the maximum difference is as high as 10%. For the Spherical Head Model, the typical difference between experimental and numerical profile factors is less than 2%. The parametric studies of the profile factor with the Reynolds number and the ultrasonic middle path chord position show differences from 1%–3%. This bias is 1.5%–2.5% for the variations of the profile factor with the axial position. The accuracy of the experimental profile factor is ±0.65%.

When the flow is turbulent (swirling), the profile factor is slightly influenced by the fluid Reynolds number; a maximum bias of 2% can be reached for particular angular and axial positions of the meter when the Reynolds number varies from 10^6–10^7.

EPRI Perspective Accurate measurement of the reactor coolant temperature, after it exits the reactor vessel (that is, the “hot-leg” temperature), is very important in the calculation of coolant enthalpy distribution in the reactor core in PWRs and in calculations used to assess plant thermal efficiency. In addition, direct measurement of the reactor coolant flow will allow direct measurement of steam generator performance and justification of continued operation at lower RCS flows resulting from plugged and sleeved steam generator tubes. The heat delivered to the steam generators can be calculated from reactor coolant flow and temperature measurements and compared to calculations of plant thermal power.

A previous EPRI project developed a prototype ultrasonic system for measuring reactor coolant temperature and flow [the Reactor Coolant System Meter (RCMS)]. The system is based on the existing technology for measuring feedwater flow using externally pipe-mounted ultrasonic systems. The measurement of reactor coolant temperature is made based on measuring the sound velocity in water. The measurement of reactor coolant flow is made based on measuring and comparing ultrasonic pulse times-of-flight downstream and upstream across the reactor coolant pipe diameter. This flow measurement technology has been developed and successfully applied for feedwater flow applications. This system is easily installed and maintained because it is externally mounted on coolant piping. As a flow measurement system, it will not be subject to inaccuracies introduced by water chemistry effects comparable to the fouling that has been experienced in venturi flow nozzles.

EPRI has developed an ultrasonic flow measurement system for this application. The accuracy of this technology is critically dependent upon knowledge of the flow velocity profile in the piping. The flow profile is typically not fully developed for this application, thus introducing measurement uncertainties that are a function of the non-uniformity of the flow profile.

Thus, the direction of improvement is to model pipe flows for various piping geometries and thermal hydraulic conditions in order to calculate flow profile factors. These factors will represent a correction to flow profile factors currently used in the instrument measurement uncertainty calculations. The EdF computational fluid dynamic software, ESTET™, was used because it is mature and is fully validated.

PROJECT

TR-107327

EPRI Project Managers: Ramesh Shankar
Revis W. James

For further information on EPRI research programs, call EPRI Technical Information Specialists, 415/855-2411.

Pipe Flow Modeling for Ultrasonic Flow Measurement Instrumentation

TR-107327

Final Report
February 1998

Prepared by
Electricité de France—Research and Development Division
6, quai Watier
78401Chatou, France

Principal Investigators
Laurent Trenty (Centrale Recherche SA)
Michel Piguet (EdF/DER—REME Branch)
Jean-Luc Rousset (EdF/DER—LNH Branch)

Prepared for
EPRI
3412 Hillview Avenue
Palo Alto, California 94304

EPRI Project Managers
Ramesh Shankar
Revis W. James

ORGANIZATION(S) THAT PREPARED THIS REPORT

Electricité de France—Research and Development Division

ORDERING INFORMATION

Price: Domestic, $5,000; International, $25,000

Requests for copies of this report should be directed to the EPRI Distribution Center, 207 Coggins Drive, P.O. Box 23205, Pleasant Hill, CA 94523, 510/934-4212.

ABSTRACT

Flow profile uncertainty is a major contributor of errors in an EPRI ultrasonic system for the measurement of reactor coolant flow and temperature. This system is called the EPRI Reactor Coolant Monitoring System (RCMS). This study discusses means to decrease the uncertainty to determine the flow profile factor that corrects the non-ideal flow profile effect. Two different piping configurations with isothermal stationary turbulent flow were modeled: the Contraction Model and the Spherical Head Model. The model-derived profile factors were compared with the experimentally-derived values from tests conducted at the Alden Research Laboratory.

Numerical profile factors were computed with an Electricité de France (EdF)—Research and Development Division (DER) software tool that models the flow with the ESTET™ [1] computational fluid dynamic code and simulates the ultrasonic flow measurement instrumentation. The obtained results show that the modeled flow profile factors for select piping configurations are in good agreement.

[1] A trademark of Electricité de France.

CONTENTS

LIST OF FIGURES

LIST OF TABLES

1

INTRODUCTION

Background

In pressurized water reactors (PWRs), direct measurement of the reactor coolant flow will allow accurate estimation of steam generator performance and justify continued operation at lower reactor coolant system (RCS) flows resulting from plugged and sleeved steam generator tubes. The heat delivered to the steam generators can be calculated from reactor coolant flow and temperature measurements, then compared to calculations of plant thermal power.

EPRI has developed a prototype ultrasonic system for the measurement of reactor coolant flow and temperature. This system is called the EPRI Reactor Coolant Monitoring System (RCMS). The system is based on existing technology for measurement of feedwater flow using an externally pipe-mounted ultrasonic system. The reactor coolant temperature is estimated from measuring the ultrasonic transit times perpendicular to flow, computing the estimated sound velocity in the fluid, and finally correlating it with temperatures based on known nomograms. Reactor coolant flow is estimated by measuring and comparing the ultrasonic pulse times-of-flight downstream and upstream—with a different set of ultrasonic transducers—across the reactor coolant pipe diameter. Then, a flow profile correction factor is applied to the data to estimate the bulk average flow. This system is easily installed and maintained because it is externally mounted on the pipe. As a flow measurement system, it is not subject to inaccuracies introduced by water chemistry effects comparable to the fouling that has been experienced in venturi flow nozzles.

Problem Statement

A substantial amount of the measurement uncertainty is caused by an incompletely developed flow profile (see Figure 1-1) and using an inappropriate flow profile correction factor. The degree to which the actual flow profile differs from a fully developed profile introduces uncertainty in the flow rate measurement. Because the actual flow profile is a function of piping configuration, the flow profile factor that corrects for this is plant specific. Consequently, a library of flow profile factors for different piping configurations would allow the flow rate measurement uncertainty to be reduced.

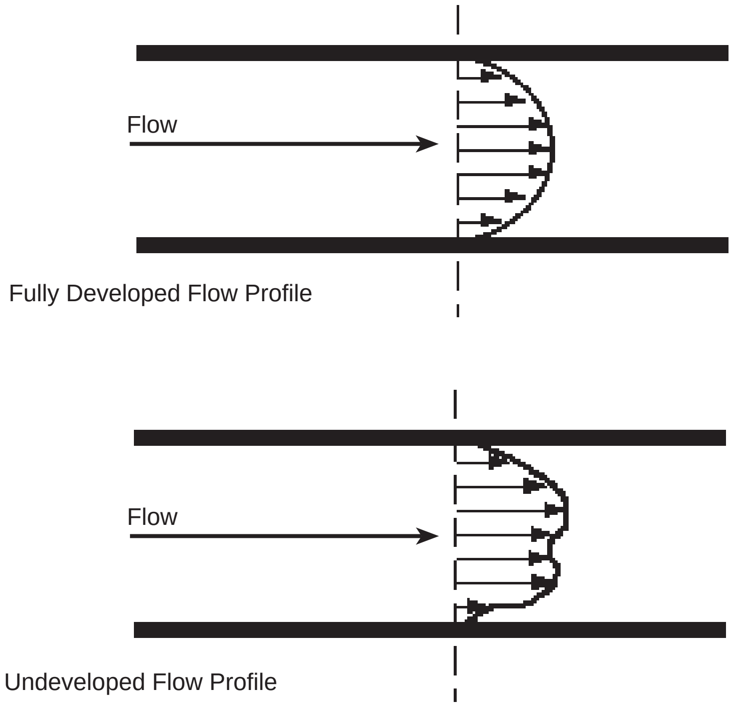

Figure 1-1
Developed Versus Undeveloped Flow Profiles

EPRI/NPG & EdF/DER Collaboration

The EPRI Energy Conversion Division (ECD) and Electricité de France Research & Development Division (EdF/DER) entered into an agreement in April 1997 to cooperate in Research and Development activities of mutual interest. A Memorandum of Understanding (MOU) addressing non-intrusive flow measurements in the PWR primary system was established [1].

EPRI/ECD and EdF/DER have both independently developed ultrasonic temperature measurement systems for this application. The systems to measure coolant flow were different; whereas EdF developed a primary flow rate measurement system based on cross-correlation of N16 γ-ray time fluctuations, EPRI developed an ultrasonic flow measurement system for this application. The accuracy of the ultrasonic measurement technology is critically dependent on the knowledge of the flow velocity profile in the piping. The flow profile is typically not fully developed for this application, thus introducing measurement uncertainties that are a function of the non-uniformity of the flow profile.

Significant improvements in the accuracy of the EPRI RCMS were possible by modeling pipe flows for various piping geometries and thermal hydraulic conditions to calculate flow profile factors precisely. These newly calculated factors would replace the nominal values used presently in the RCMS, and potentially lead to reduced measurement uncertainty.

It was decided that the EdF Computational Fluid Dynamic (CFD) software, ESTET, was used because it is mature and had been validated. In addition, the EdF Reliability, Measure, and Testing Branch (REME) of EdF / DER developed an integrated tool coupled to ESTET for the modeling of flows and the simulation of differential pressure devices and ultrasonic flowmeters.

The purpose of the work within the MOU was to conduct a feasibility study on specific piping configurations to demonstrate validity of the modeling approach. EPRI identified piping configurations developed at the U.S.-based Alden Research Laboratory to simulate flow conditions at a U.S. nuclear plant to be modeled under the project. These configurations were selected because they allowed a comparison between experimental and modeling data.

Approach

The project was structured in four tasks:

Task 1—Selection of Piping Configurations to Analyze

A specific piping configuration was chosen based on the ability to compare experimental and modeling data. When actually used, the model should compute a plant-specific flow profile factor for each configuration for which an RCMS is to be installed.

Task 2—Flow Profile Factor Analysis

The ESTET CFD code was used to simulate the flow conditions in the chosen configuration. A flow profile factor that represents the difference between the ultrasonic pulse time-of-flight under fully developed flow conditions and actual flow conditions was calculated.

Task 3—Sensitivity Studies

Sensitivity studies were performed on all significant input variables to determine the most important factors in determining the flow profile factor and to identify the most important plant-specific conditions that must be modeled. The objective of this task was to determine the extent to which flow profile factors can be calculated.

Task 4—Study of another Configuration

Because of time and budget constraints after the initial analysis, another configuration could not be addressed in the present MOU. However, the two ARL configurations were completely addressed.

Organization

EdF subcontracted the computer analysis work to one of the research laboratories of the *Ecole Centrale*, which is one of the premier French engineering establishments. EdF was responsible for the project and reviewed and analyzed all computer analyses to ensure the validity of the modeling assumptions and the consistency of results. The project duration was from April 1997–November 1997.

2

PIPE FLOW MEASUREMENT AND MODELING

Flow Profile Factor Computation

The volumetric flow rate through a pipe is the fluid velocity vector parallel to the axis of the pipe integrated over a plane normal to the axis of the pipe. The volumetric flow rate is determined by multiplying the diametral axial velocity by the area of the pipe and a profile factor that relates the measured diametral velocity to the velocity averaged over the entire pipe cross-section:

(Eq. 1)

where,

Q	=	Volumetric flow rate
PF	=	Hydraulic profile factor
ID	=	Inside diameter of the pipe
V_{axial}	=	Average axial flow velocity measured along the diametral chord

If the velocity profile is fully developed—for example, at distances more than 5–10 diameters from the pipe fixture on a long, straight pipe section—the cross-sectional average axial velocity is about 0.94 times the diametral average velocity measured by the flowmeter; that is, the profile factor is 0.94.

Under industrial conditions, where very few straight lengths are available up- or down-stream of the meter, the flow is non-ideal (that is, not fully developed). Also, the profile factor has to be determined to correct a systematic bias that represents a small but significant percentage of the measured value. EdF tests showed that the flowmeters placed less than five times the diameter measure flow with errors 3%–5%. Also, for some geometrical configurations, such as expanders, the errors can be up to 30% [2].

The profile factor is typically determined by an experimental test using a flow model that hydraulically simulates the actual installation. The test consists of ultrasonically measuring the velocity and noting the fluid accumulation in a weight tank over prescribed time intervals. The experimentally derived flow profile factor is simply the ultrasonically measured velocity divided by the experimentally derived velocity obtained from the measured accumulation per unit time, according to Equation 1. The profile factor (PF) value is defined as:

where,

PF = Profile factor

$V_{section}$ = Axial velocity averaged over the pipe cross-section (equal to the volumetric flow rate divided by the cross-sectional area where the flow rate is measured in the experimental approach or the code imposed flow rate in the numerical approach)

V_{axial} = Average axial velocity in the diametral measurement plane of the RCMS (measured with the meter in the experimental approach, computed in the numerical approach)

The profile factor can also be determined by a numerical modeling of the hydraulic circuit and the computation of the average diametral axial velocity. The two approaches are examined in this document.

Alden Research Laboratory Configurations

Interest in the RCMS was initially expressed by the Tennessee Valley Authority’s (TVA) for use at their Watts Bar nuclear plant and by Rochester Gas and Electric at their R. E. Ginna nuclear plant. To determine profile factors for the Watts Bar RCS loops, a scaled piping model was constructed at the Alden Research Laboratory (ARL). The basic test loop for the ARL hydraulic test represents the bottom of a steam generator modeled by a spherical head with a discharge nozzle. It is called the Spherical Head Model.

In order to quantify profile factor sensitivity at the metering location to the shape of the velocity profile entering the 40° elbow, a second model was constructed using a concentric 24"-to-16" reducer immediately upstream of the 40° elbow. This model is called the Contraction Model.

Weight tank runs were performed at ARL to determine experimental profile factors for these two configurations. Profile factors calculated are based on volumetric flow rates from the Caldon Leading Edge Flowmeter (LEFM) and the ARL weight tank. The LEFM is an externally mounted acoustic flowmeter that is used in feedwater flow measurement applications and operates on the same acoustic principles as the RCMS providing accurate measurement of the axial velocity (V_{axial}). The quantity ($V_{section}$) is determined by the gravimetric method from the ARL weight tank measurements.

The uncertainty in the profile factors determined from the ARL tests arises from the uncertainty in the weight tank measurements and in the LEFM used in the tests, that is, metering section dimensions, wedge and pipe acoustic properties, time measurement, and so on). The measured uncertainties were 0.25% and 0.60%, respectively [3] (Appendix C.3, Paragraph G). Because the errors are from random, independent processes—that is, the ultrasonic measurement is not affected or influenced by the weight tank measurements—the overall uncertainty is the square root of the sum of the squared errors, 0.65%.

Experimental and Modeling Data

The profile factor was computed for:

- Different axial positions of the meter before the 40° elbow, at 1.6 and 4.8 pipe diameters downstream from the downstream flange of the elbow.
- Different angles of the acoustic plane orientation (from -90° to +90°)
- The flowmeter at different distances from the 24"-to-16" reducer (in the case of the Contraction Model)
- Varying Reynolds number

In addition, a sensitivity study was performed to evaluate the influence of numerical parameters on the profile factor calculation. The following parameters were evaluated:

- Grid size
- Reynolds number
- Inlet velocity conditions
- Turbulence models
- Physical characteristics of the fluid (temperature and pressure)

EdF/DER Tool

This study was carried out using an EdF / DER tool (recently developed by the REME branch). This tool is built around the ESTET code developed at EdF's *Laboratoire National d'Hydraulique* (see Figure 2-1).

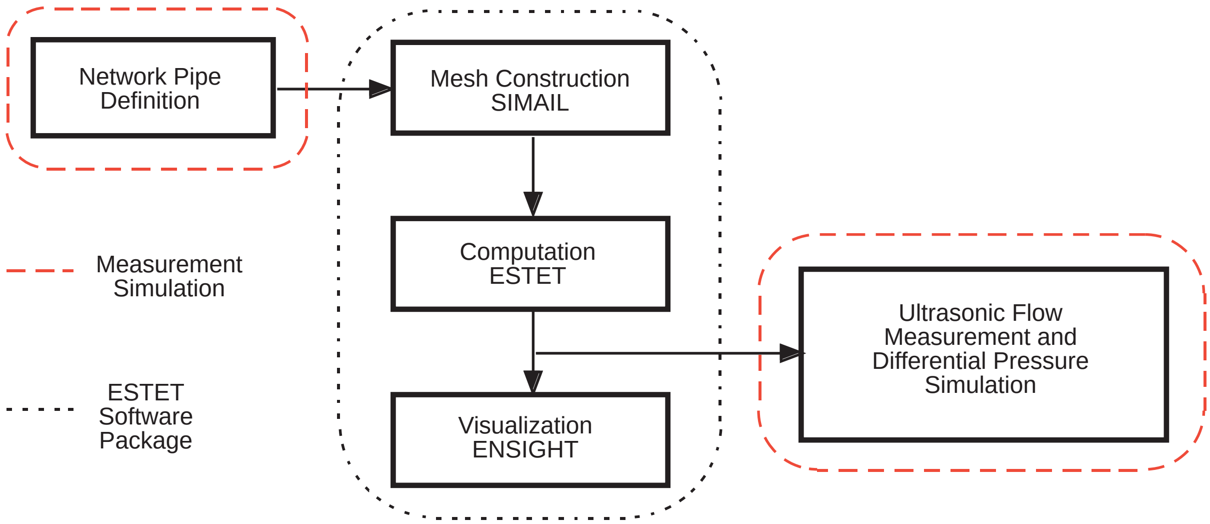

Figure 2-1
EdF/DER Tool for Flow Rate Measurement Simulation
See appendix B for color representation

ESTET's input section to define the mesh construction for specified geometries is performed by SIMAIL™, a 3-D structured or non-structured mesh construction software. It was developed by Simulog (France). ENSIGHT is a post-treatment software developed by Computational Engineering International—U.S. (CEI). These two software routines are part of the ESTET package. The dashed rectangles show the added part to the ESTET code. The first part (network pipe definition) allows the user to easily construct and mesh the pipe network without having knowledge of the SIMAIL software. The second part (ultrasonic flow measurement and differential pressure simulation) is the principal interest of the tool. It allows the simulation of experimental ultrasonic flow measurements and differential pressure devices (orifice plates).

The tool runs on a Hewlett-Packard 700 station, system 9.x, and ESTET can be executed either on a workstation or on a CRAY®[2] computer.

Modeling Pipe Flow

The flow modeling is achieved with ESTET, which is a 3-D fluid mechanic code using finite difference / volume numerical methods. The transport equations are solved on a structured mesh. In this study, the Navier Stokes equations are solved on a curvilinear mesh with finite volume method. The convection model is based on a quick-upwind convection scheme (superior order scheme).

[2] Cray is a subsidiary of Silicon Graphics, Inc.

The flow is modeled to be in 3-D, isothermal, stationary, and turbulent, which can be simulated using one of the three approaches:

- The k-ε model
- The Reynolds stress model
- The RNG model with a logarithm wall-function for the wall-boundary conditions

The computer runs were performed on a CRAY C98 computer.

Measurement Instrumentation Simulation

A post treatment software allows to simulate the ultrasonic flow measurement instrumentation and to calculate the mean velocity on an ultrasonic chord. The profile factor is calculated comparing the mean velocity in the pipe section to the mean velocity on the chord. In this study, the different parameters for the calculations of the profile factor are the same like the experimental Contraction Model and Spherical Head Model (diagonal path orientation, axial meter positions, and angular meter positions).

It is assumed that the axial positions are marked from the middle of the acoustic path and that the angle between the acoustic path and the flow axis is constant and equal to 45° (see Figure 2-2).

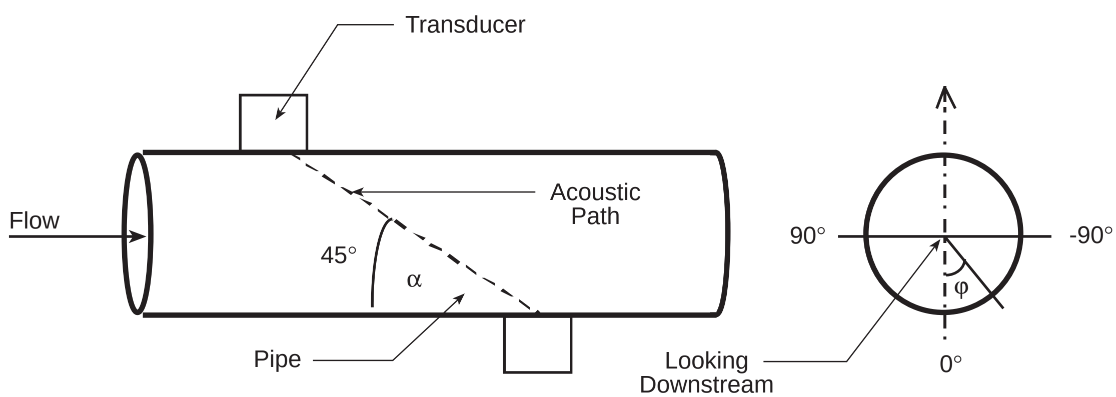

Figure 2-2
Ultrasonic Diagonal Path Position and Orientation

3

CONTRACTION MODEL

Section Overview

This section describes results obtained for the Contraction Model to simulate the effect of a reducer. Flow modeling results were acquired using the ESTET 3.2.6 version. Because the construction and the mesh of a reducer is not yet available in the EdF tool library, the Contraction Model mesh is directly performed with SIMAIL. This case was studied first, which allows the best parameters for the study to be determined: numerical and geometrical parameters for the computer runs (that is, numerical schemes, reference time step, Courant and Arakawa numbers, number and distribution of grid nodes, and so on).

Pipe Model Parameters

In order to minimize the total number of nodes, the numerical Contraction Model is composed of a part of the reducer followed by a 40° elbow and an 8' 6" straight pipe with a 16" diameter. The reducer is 20" long. Figure 3-1 shows the Contraction Model mesh generated from SIMAIL. The mesh is curvilinear comprised of 194,145 nodes ($43 \times 43 \times 105$ I-, J-, K-planes). Figure 3-1 shows the grids used on the reducer section.

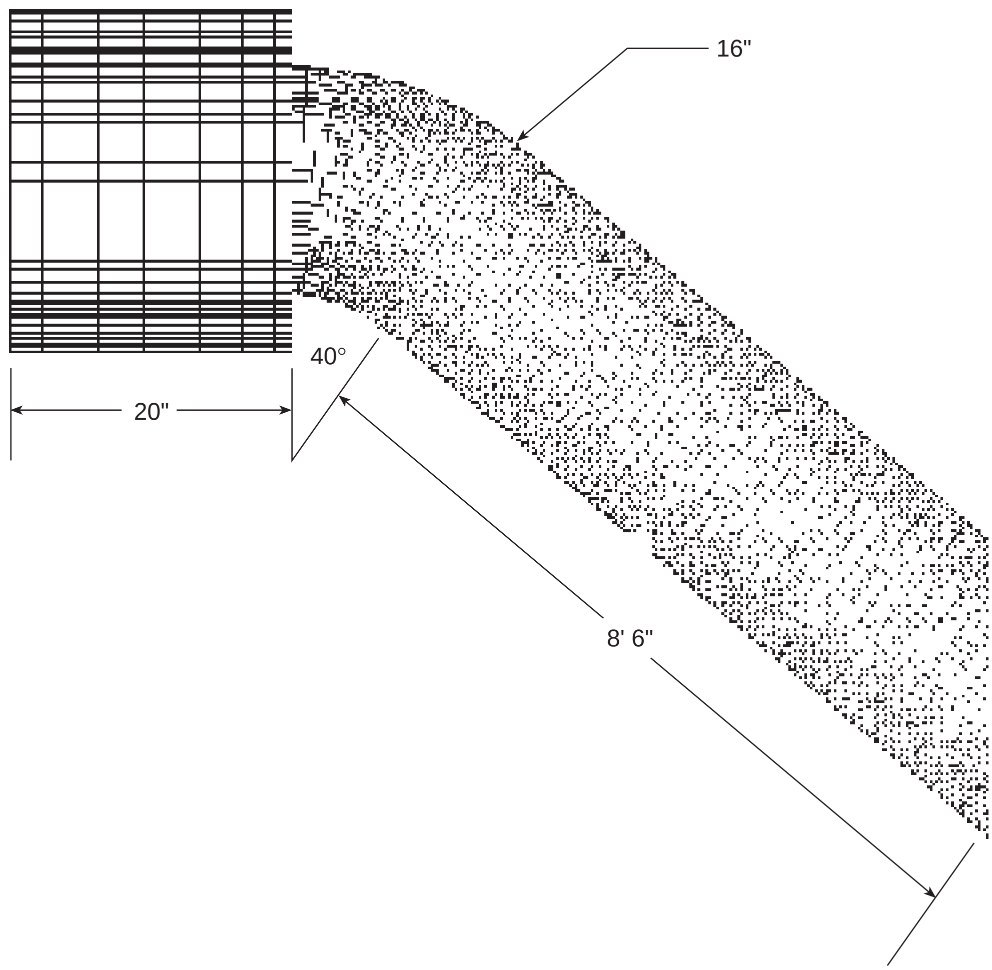

Figure 3-1
Geometry and Mesh of the Contraction Model

Figure 3-2 presents a mesh section (43[I] × 43[J]) for the 24" reducer that is generated from the 16" pipe mesh. The grid presents four singular areas where strong non-orthogonalities are found in the cells (at 45° of each quarter of the grid).

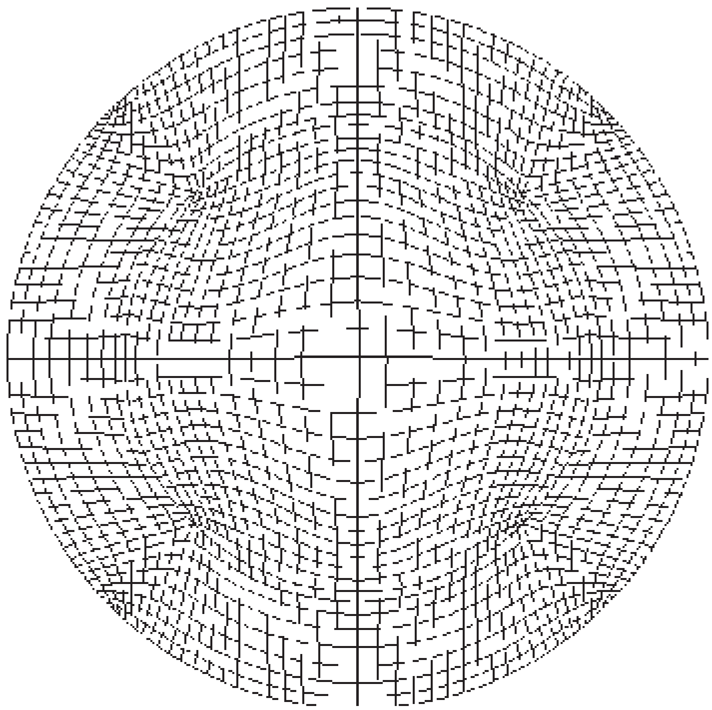

Figure 3-2
The 24"-to-16" Reducer Mesh Section of the Contraction Model

All the computations assume an isothermal flow at 560.9°K (550°F) with a pressure equal to 1.55×10^7 Pa (2.25×10^3 psia). At the inlet of the 24" diameter reducer, an axial profile velocity is imposed. This profile is calculated according to the following function:

(Eq. 2)

where,

V(r) = Inlet axial velocity

V_m = Axial velocity on the axis calculated from the Reynolds number and the pipe inlet hydraulic diameter

r = Radial position

R = Pipe inlet inside radius

Re = Reynolds number

In the results presented hereafter, the Reynolds number is equal to 10^{+6}, which corresponds to a velocity of 0.26 m/s (10.2 in./s). The 16" pipe outlet is considered to be an open boundary. Boundary conditions at the pipe wall require that the velocity along the ID be calculated using a logarithm wall-function [4].

Numerical Results

The results discussed and pictorially displayed in this section show the behavior of the fluid flow in the Contraction Model. Figure 3-3 illustrates the longitudinal velocity profile along the pipe in the middle vertical plane. At the outlet of the elbow, a detachment of the flow can be seen. The maximum velocity in the pipe is less than 0.70 m/s (27.6 in./s). The flow is not stable yet at the outlet of the 16" pipe diameter (≈ 6.4D). In Figure 3-4, the velocity is projected on two pipe sections perpendicular to the flow direction: at the inlet of the 40° elbow and at the outlet of the 40° elbow. There is almost no swirl and the fluid presents a vertical symmetry plane.

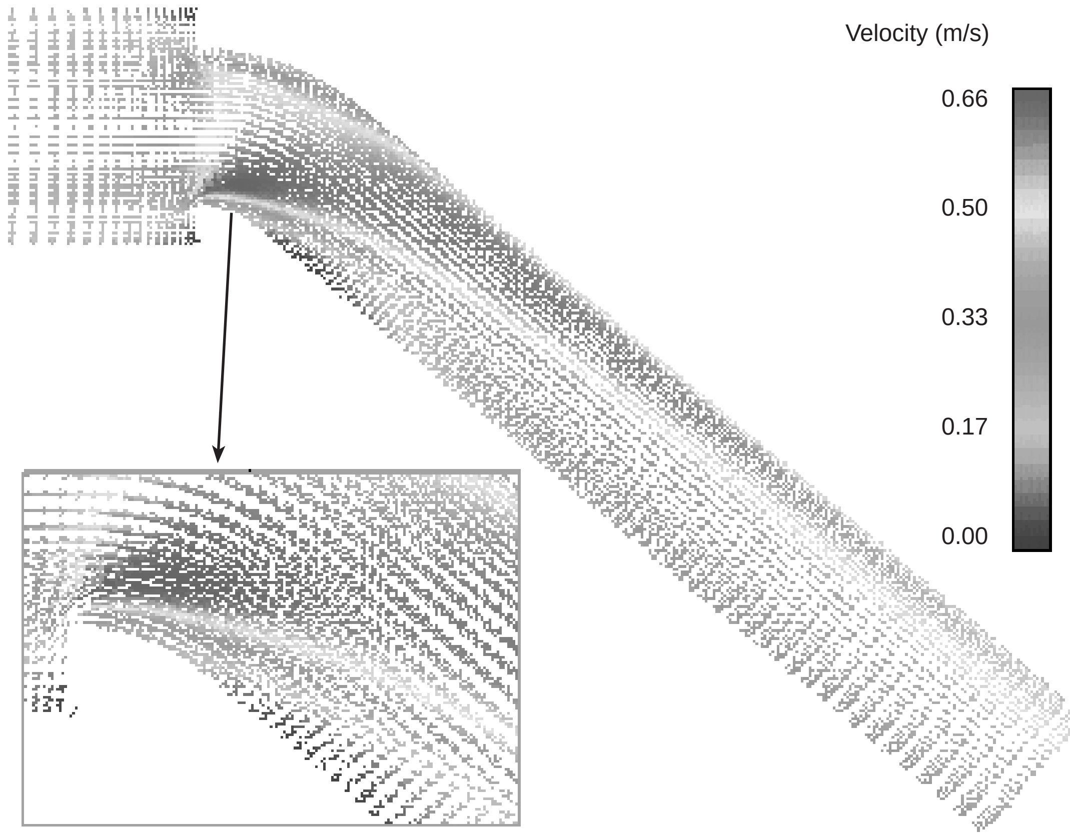

Figure 3-3
Longitudinal Velocity Profile in the Middle Vertical Plane (Contraction Model)
See appendix B for color representation

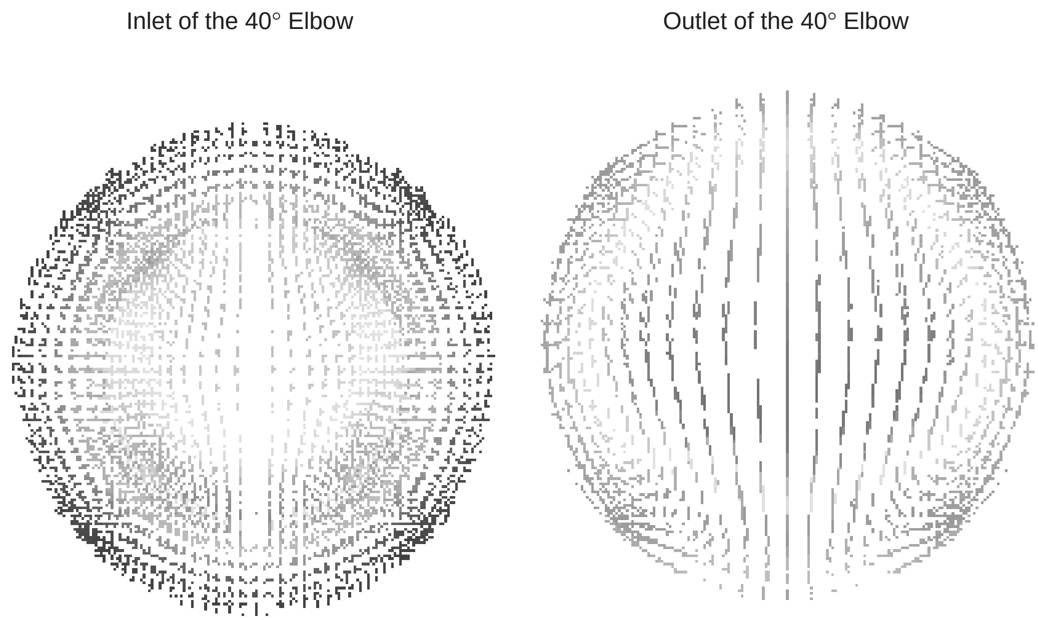

Figure 3-4
Tangential Velocity Profiles in the Pipe Section at the Inlet and Outlet of the 40° Elbow (Contraction Model)
SEE APPENDIX B FOR COLOR REPRESENTATION

Figure 3-5 shows the pressure distribution for the configuration. The model clearly shows that the pressure is almost constant in the pipe: the pressure gradient is only equal to 1.70 x 10^2 Pa (2.47 x 10^{-2} psia). Figures 3-6 and 3-7 show the pressure field through two different pipe sections perpendicular to the flow direction. In Figure 3-7, which corresponds to the outlet of the 40° elbow, the low pressure is due to the detachment of the flow.

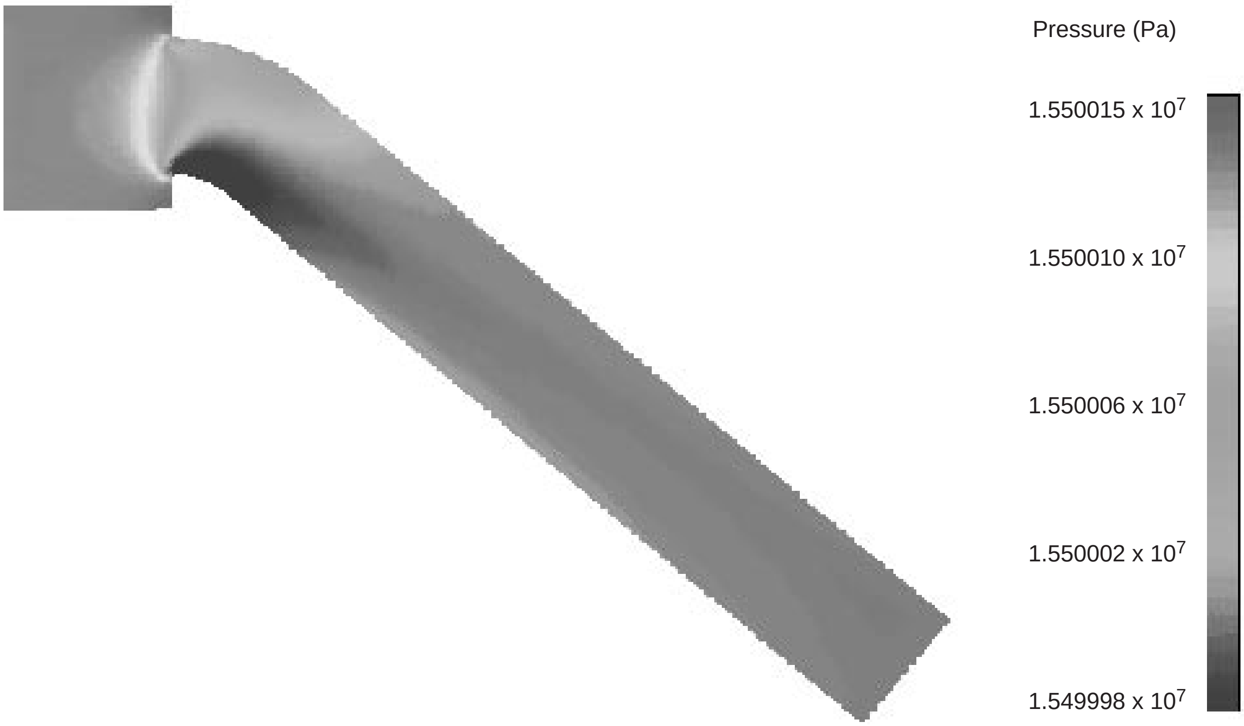

Figure 3-5
Pressure Field in the Middle Vertical Plane (Contraction Model)
SEE APPENDIX B FOR COLOR REPRESENTATION

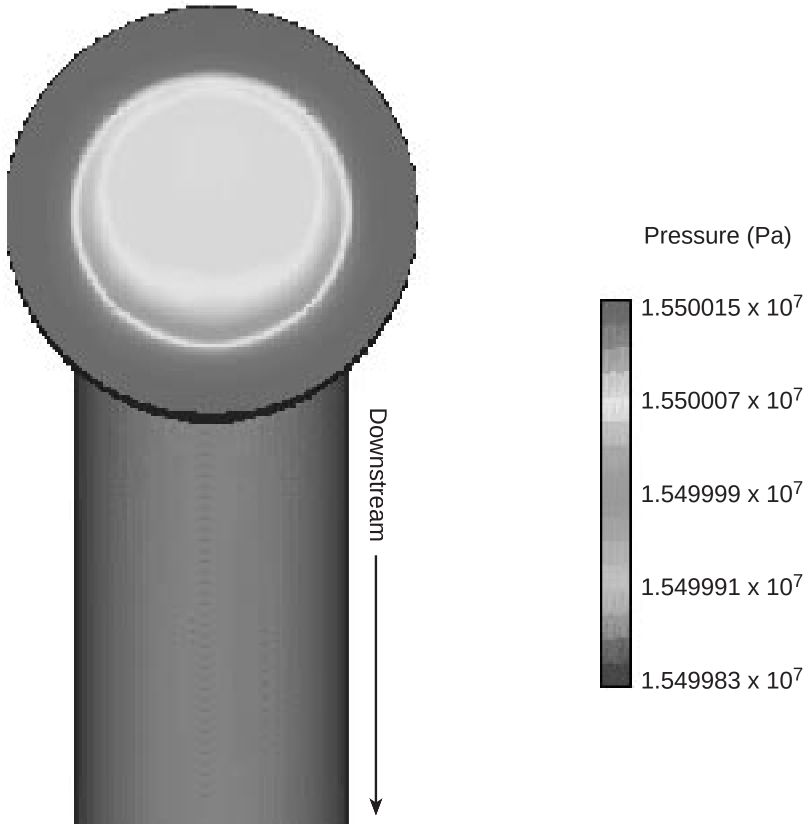

Figure 3-6
Pressure in the Pipe Section at the Inlet of the 40° Elbow (Contraction Model)
SEE APPENDIX B FOR COLOR REPRESENTATION

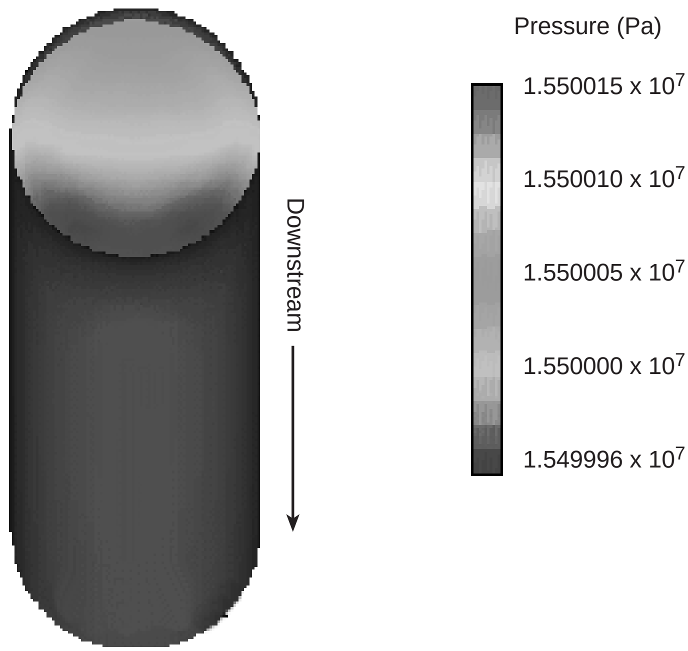

Figure 3-7
Pressure in the Pipe Section at the Outlet of the 40° Elbow (Contraction Model)
SEE APPENDIX B FOR COLOR REPRESENTATION

These results correspond to a steady state; there is no temporal variation for all the computed variables although the drift of the turbulent variables (k-ε) does not go to zero. This phenomenon is due to limitations of the ESTET model used for this configuration. As the ESTET model requires a single-block mesh, it is not possible to create a mesh in this domain with enough freedom. For example, this type of mesh does not allow configuring of a fine mesh at the wall without creating greater non-orthogonality of the cells. This constraint affects the prediction of the wall velocity. This situation is improved on the ESTET 3.3.2 version that is used for the Spherical Head Model.

Profile Factor Comparisons

The profile factors were calculated for two axial positions (1.6D and 4.8D) from the outlet of the 40° elbow and an acoustic path angle varying from -90° to +90° under the assumptions described in Section 2.

In Figure 3-8, the profile factor is plotted as a function of the angular position of the ultrasonic flow measurement transducer. The profile factor evaluated with the EdF tool is compared to the EPRI experimental data.

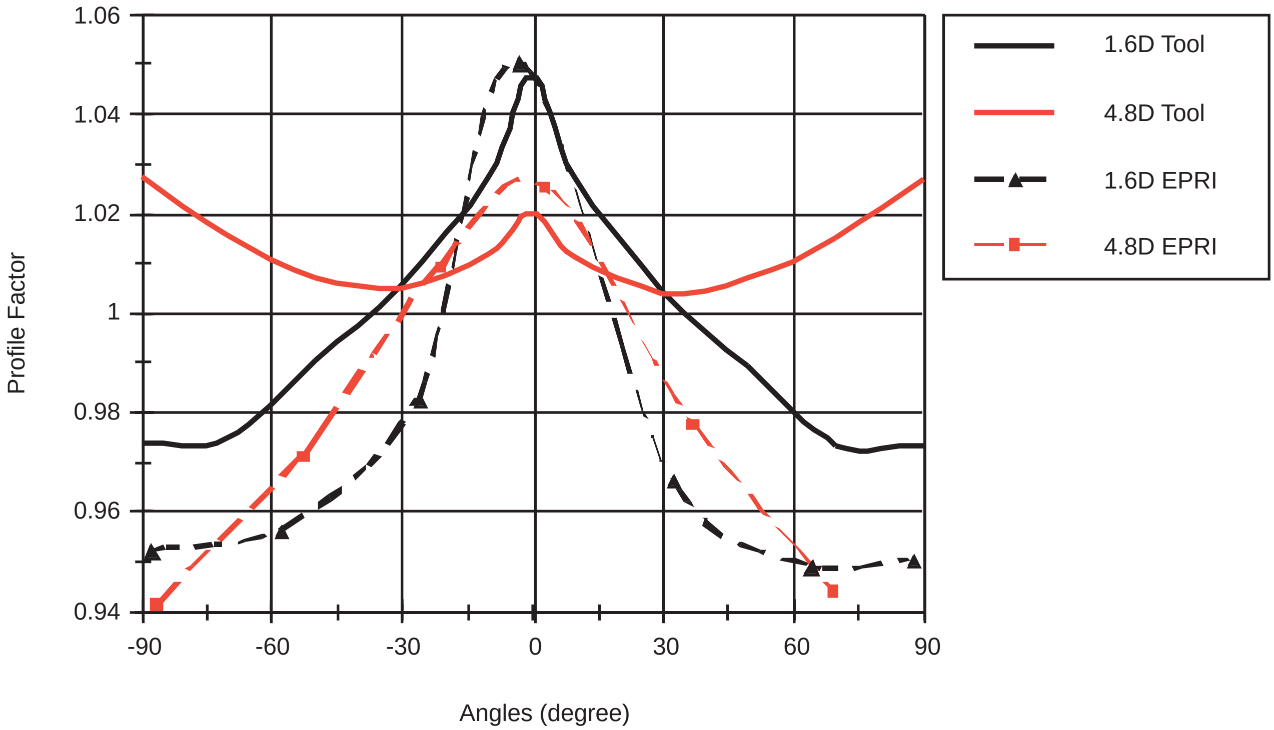

Figure 3-8
Variations of the Profile Factor with the Angle (Contraction Model)
("Tool" Stands for EdF Tool Results and "EPRI" Stands for EPRI Experimental Data)
SEE APPENDIX B FOR COLOR REPRESENTATION

At the 1.6D axial position, the numerical results are in good agreement with the experimental data: the difference between experimental and numerical PF is from 0% at 0° to a maximum of 3% at ±60°.

At the 4.8D axial position, the simulation tracks the EPRI measurement results accurately in the range -30° < θ < +30°: from 0% at 30° to a maximum of 3% at 0°. Outside of this range, that is, |θ| > 30°, there is not good agreement between the modeled PF and experimental data: a maximum of 10% is reached at ±90°. This could be due to incorrect estimation of the computed wall velocity, which is possibly due to the use of ESTET 3.2.6 in curvilinear mesh.

Figure 3-9 shows the variations of the profile factor as a function of Reynolds number. The profile factor is almost not influenced by the variation of the Reynolds number, similar to the experimental results. An almost constant difference can be noticed between the modeled and experimental PFs: about 1% for the -2° angular position and between 2% and 3% for the +88° angular position. However, it must be emphasized that the axial position for this case is not exactly known. For the simulation, the result is given for an assumed position of 1.6D.

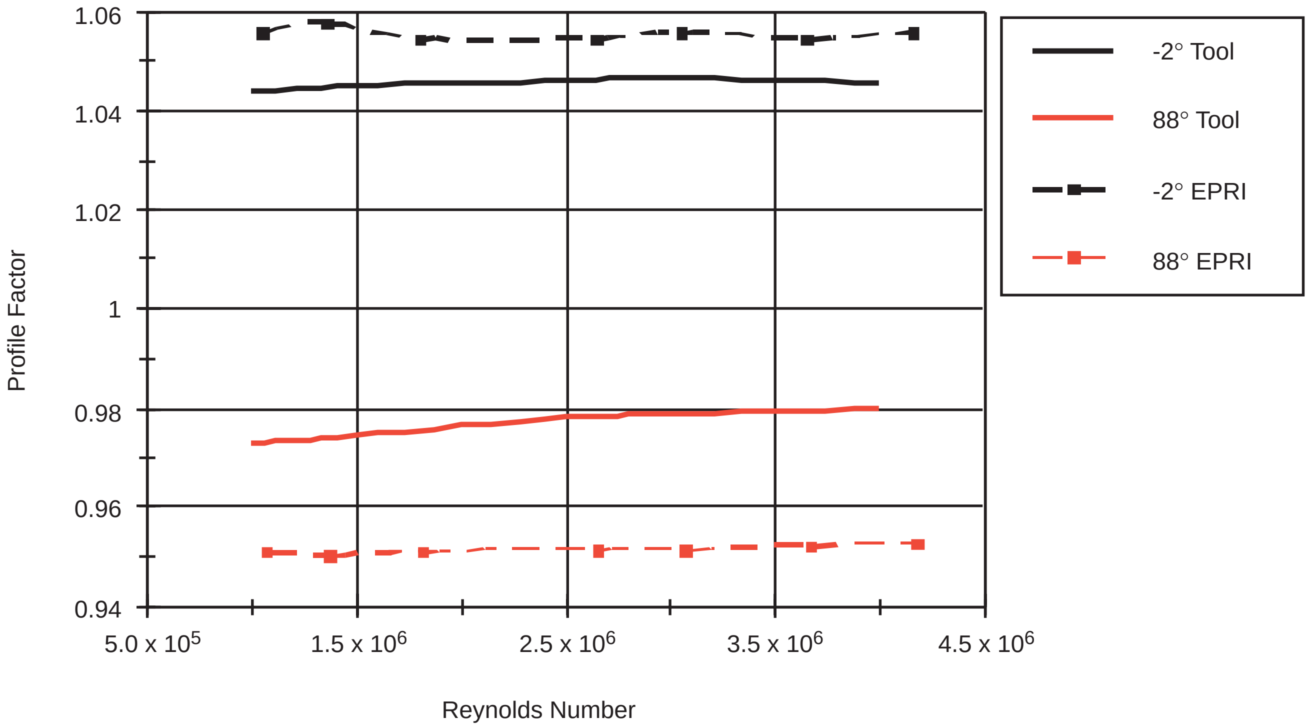

Figure 3-9
Variations of the Profile Factor with the Reynolds Number (Contraction Model)
SEE APPENDIX B FOR COLOR REPRESENTATION

4

SPHERICAL HEAD MODEL

Section Overview

The Spherical Head Model simulates the bottom of a steam generator and produces results that are more directly representative of practical primary coolant flow conditions. Therefore, this model is likely to be more interesting than the Contraction Model. The later version of ESTET model (version 3.3.2) was used. In addition to the standard test (Reynolds number influence), the influence of the inlet axial velocity profile and the temperature and pressure references [300.15°K (80.6°F) and 1.013 x 10^5 Pa (1.47 x 10^1 psia)] were studied.

The geometrical configuration defined in Figure 4-1 takes into account the 24" diameter inlet pipe closed by a spherical head. A 16" diameter pipe is in continuation of the Spherical Head.

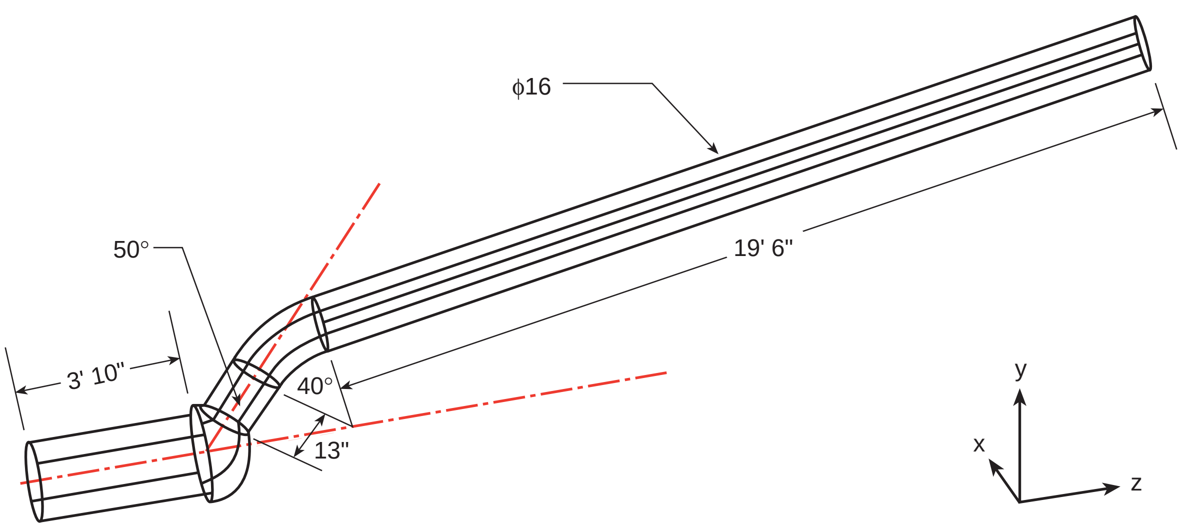

Figure 4-1
Geometry of the Spherical Head Model
SEE APPENDIX B FOR COLOR REPRESENTATION

Numerical Characteristics

Because of the geometrical complexity of the model, the mesh is generated with more powerful CAD software: ICEM™ (developed by Control Data). Figure 4-2 shows the Spherical Head Model grid in the vertical plane. Like the Contraction Model, the mesh is curvilinear and single-block. It is made up of 95,550 nodes ($21 \times 25 \times 182$ I-, J-, K-planes). Figures 4-3 and 4-4 present the mesh sections ($21[I] \times 25[J]$) at the inlet of the sphere and in the 16" diameter pipe, respectively.

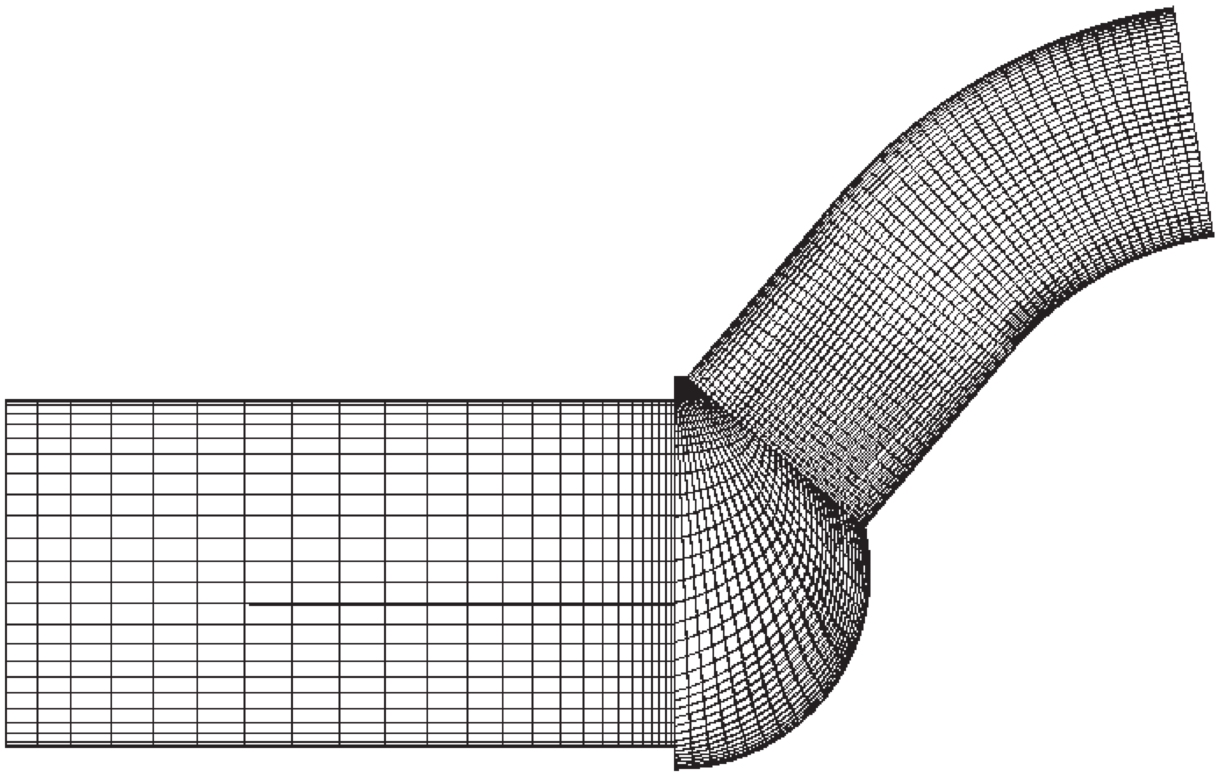

Figure 4-2
Spherical Head Model Mesh in the Vertical Plane (Part of It)

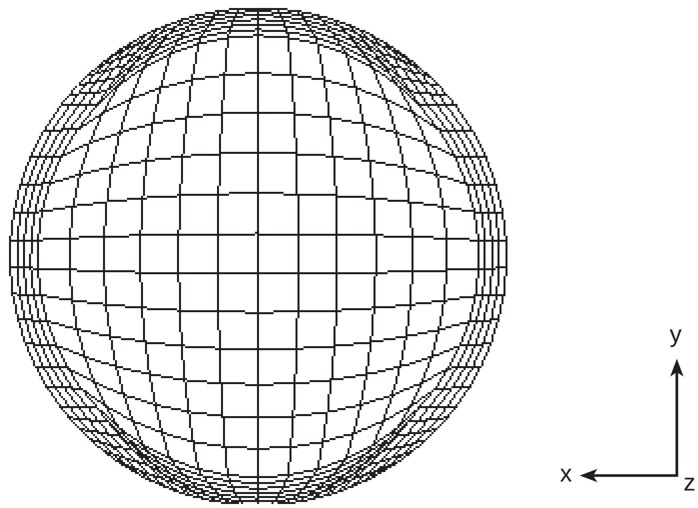

Figure 4-3
Spherical Head Model Mesh Section at the Inlet of the Sphere

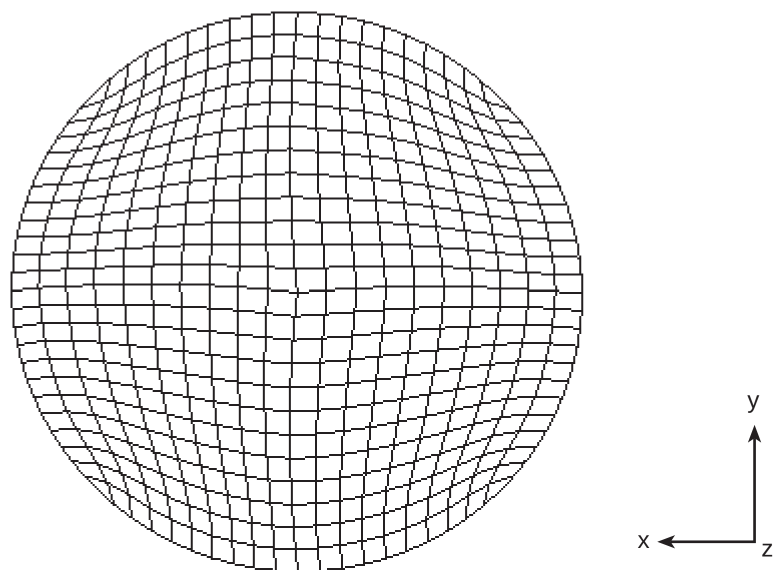

Figure 4-4
Spherical Head Model Mesh for the 16" Diameter Pipe Section

An isothermal flow set to 560.9°K (549.95°F) with a referential pressure equal to 1.55×10^7 Pa (2.25×10^3 psia) is assumed, which is similar to the Contraction Model. A computation is carried out with a constant temperature equal to 300.15°K (80.6°F) and a pressure set to 1.013×10^5 Pa (1.47×10^1 psia). This case allows the evaluation of the influence of physical parameters on the profile factor. At the inlet of the 24" diameter reducer, an axial flat velocity profile is imposed and calculated as a function of the Reynolds number. For a fixed Reynolds number, another computation is performed with an inlet turbulent profile (parabolic) to evaluate its influence on the profile factor results (refer to Equation 2, which is used to calculate this profile). The 16" pipe outlet is considered as an open boundary. At the pipe wall, the velocity is determined from imposing boundary conditions using a logarithm wall-function.

Numerical Results

All the results presented hereafter are obtained with a flat inlet velocity profile for a Reynolds number equal to 10^6. Figures 4-5 and 4-6 depict the pressure and velocity on a vertical plane, respectively. The pressure is almost constant with only a slight pressure variation equal to 3.70×10^2 Pa (5.37×10^{-2} psia). At the outlet of the sphere, the narrowing of the geometry divides the flow into two parts. The velocity increases at the bottom of the pipe and decreases at the top of the pipe. After the 40° elbow, the fluid is still divided into two parts: one part is in the middle of the pipe where the velocity increases. The maximum velocity is about 0.75 m/s (29.5 in./s).

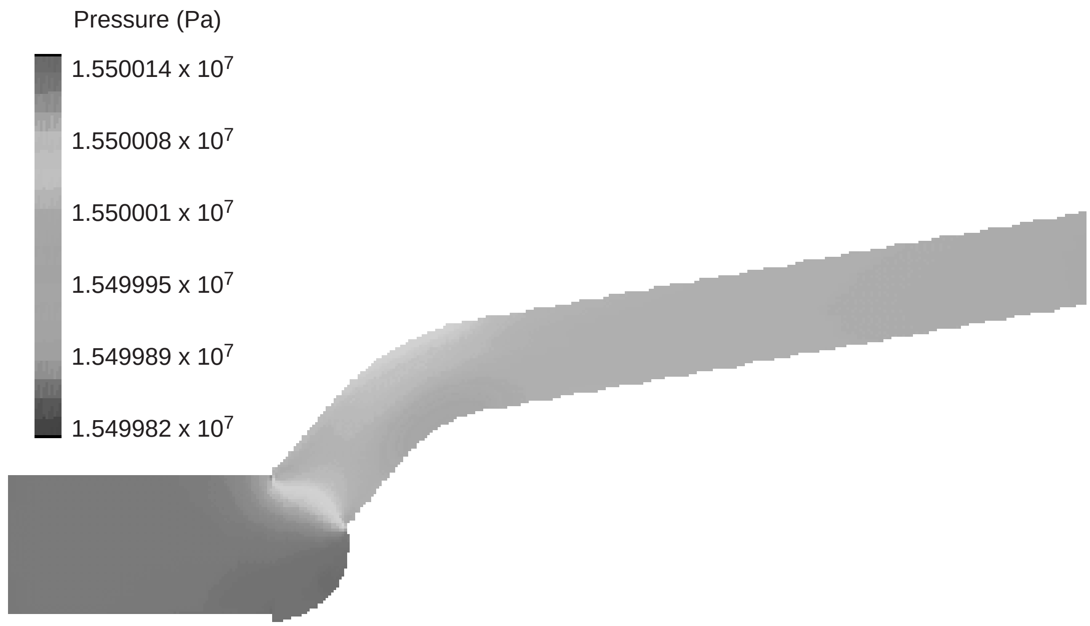

Figure 4-5
Pressure Field in the Middle Vertical Plane (Spherical Head Model)
See appendix b for color representation

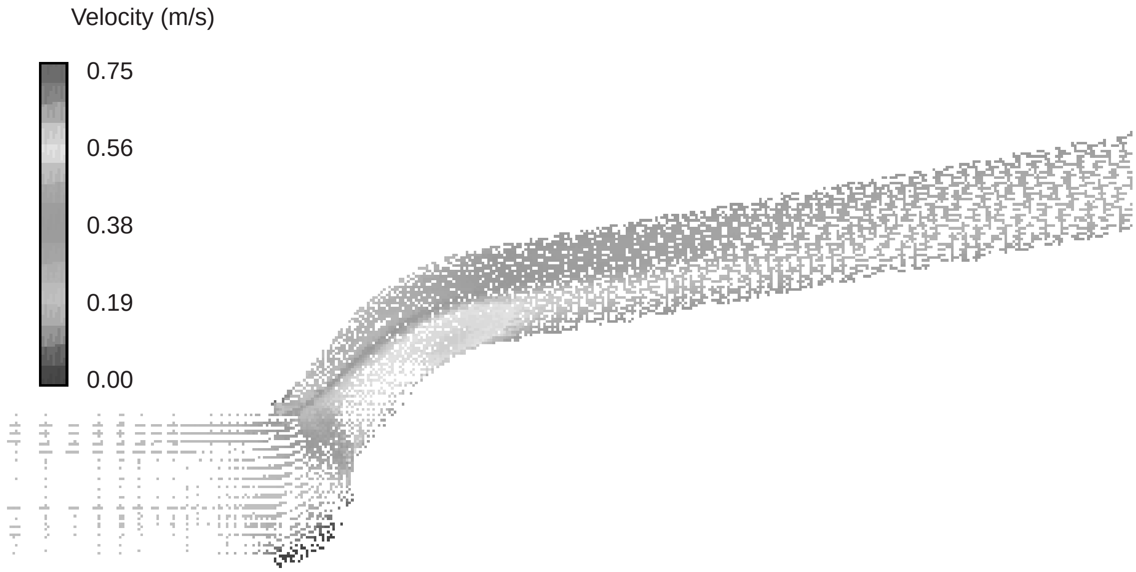

Figure 4-6
Velocity in the Middle Vertical Plane (Spherical Head Model)
See appendix b for color representation

Figure 4-7 shows the pressure on different pipe sections. All pipe sections are looking downstream (that is, the flow is into the page). In Figure 4-8, the tangential velocity is plotted on the same pipe sections. In contrast to the Contraction Model, where there is almost no swirl in the fluid, the tangential velocity in the Spherical Head model is not insignificant. Figure 4-9 shows the turbulent viscosity.

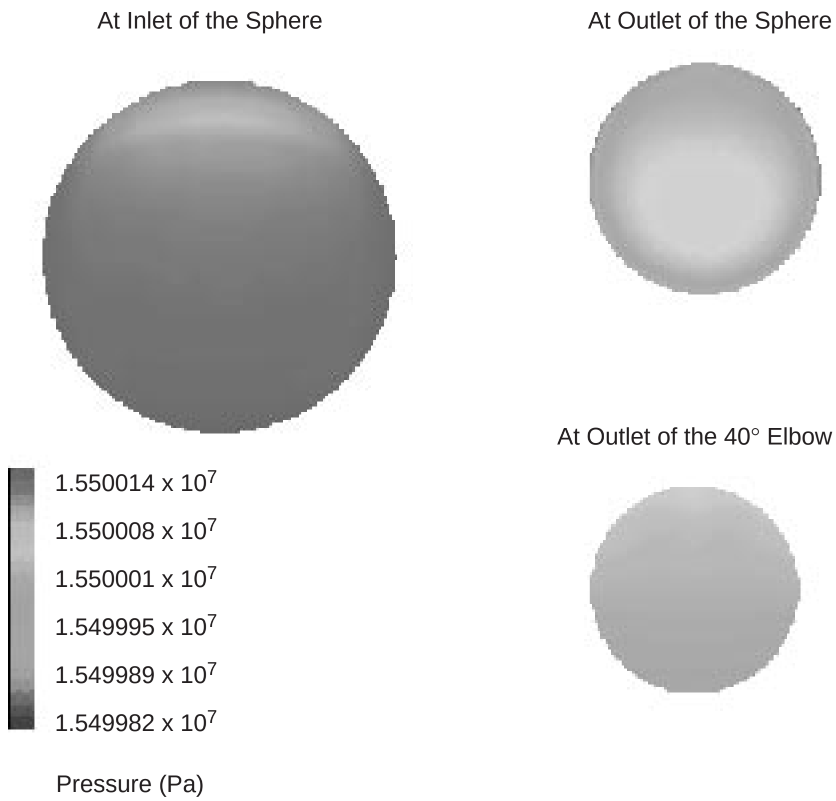

Figure 4-7
Pressure Field in Pipe Sections Perpendicular to the Flow (Spherical Head Model)
See appendix b for color representation

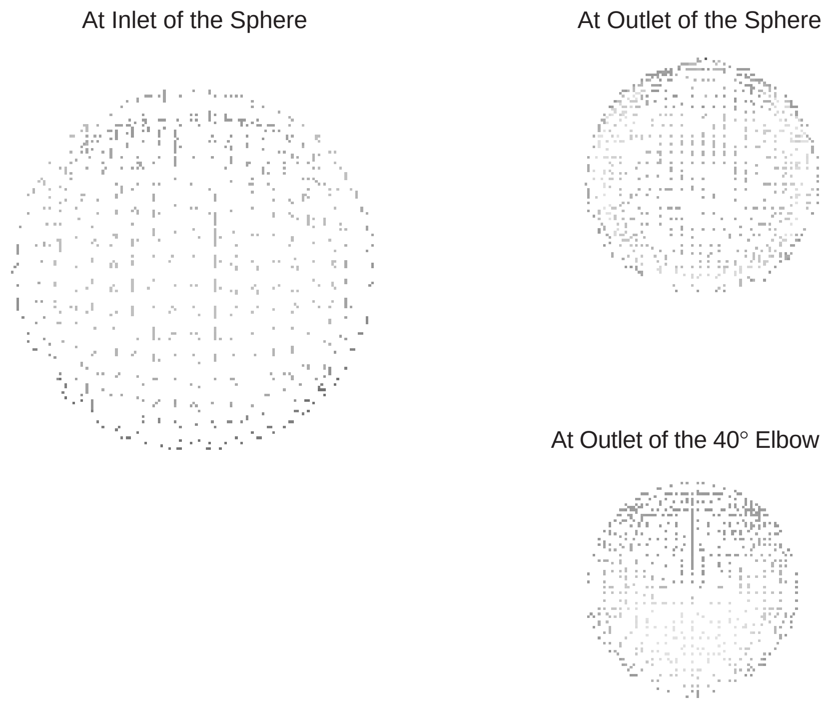

Figure 4-8
Tangential Velocity in Pipe Sections Perpendicular to the Flow (Spherical Head Model)
SEE APPENDIX B FOR COLOR REPRESENTATION

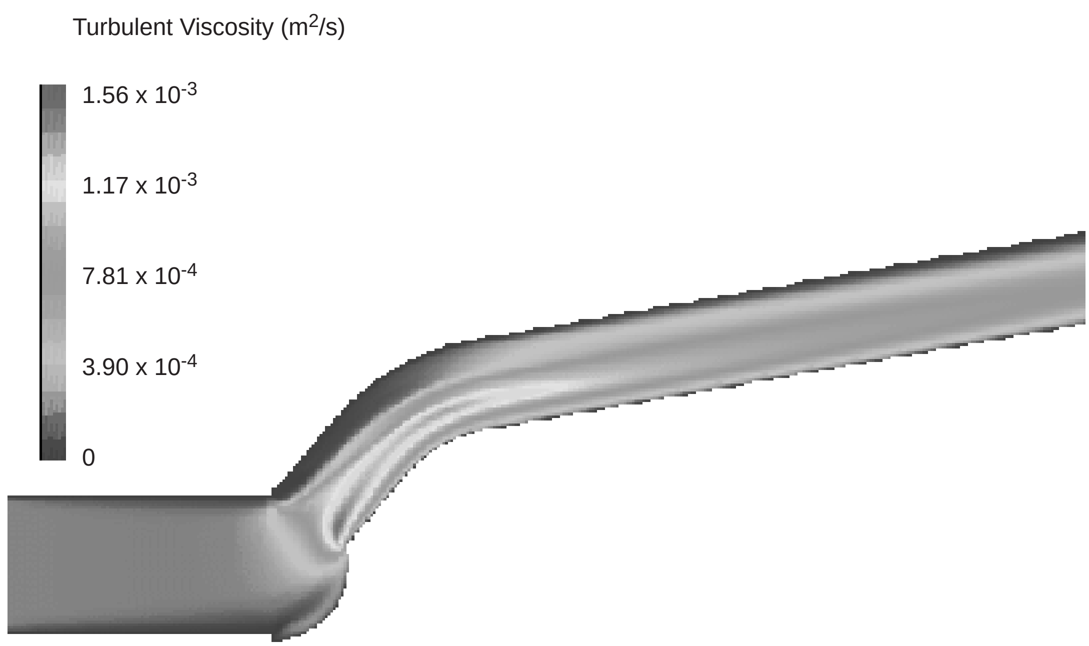

Figure 4-9
Turbulent Viscosity in the Middle Vertical Plane (Spherical Head Model)
SEE APPENDIX B FOR COLOR REPRESENTATION

Profile Factor Comparisons

The profile factors presented in this section are calculated from an isothermal flow at 560.9°K (549.95°F) with a referential pressure of 1.55 x 10^7 Pa (2.25 x 10^3 psia). The imposed inlet velocity profile is flat.

Figure 4-10 presents the angular variations of the profile factor. The simulation results are in good agreement with the experimental data: the tendency is well predicted by the tool and the difference between experimental and numerical PF is lower than 2%, except in the region of 0° at 1.6D where a difference of 6% is noticed between experimental and numerical results. The difference at the 0° angular position could be caused by an over estimation of the axial velocity at the outlet of the sphere. This error might be reduced with a refinement of the sphere grid.

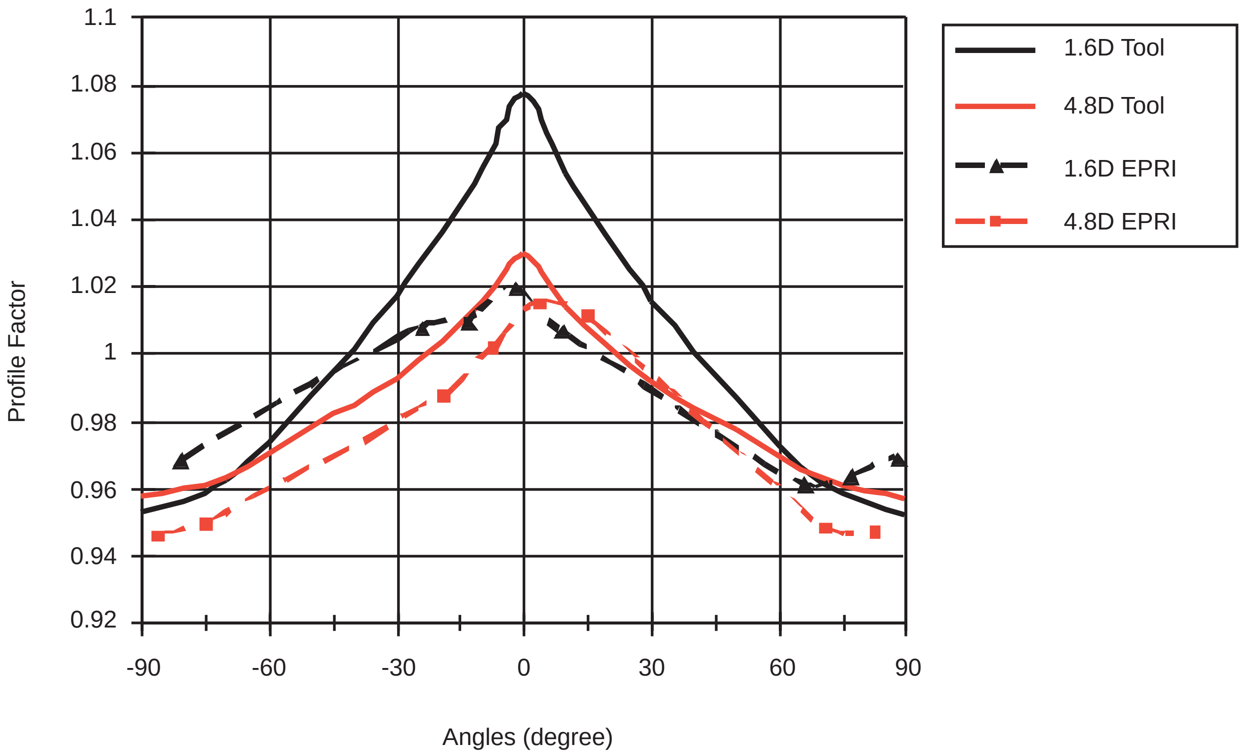

Figure 4-10
Variations of the Profile Factor with the Angle (Spherical Head Model)
("Tool" Stands for EdF Tool Results and "EPRI" Stands for EPRI Experimental Data)
See appendix b for color representation

Figure 4-11 shows the profile factor variation with the Reynolds number. This variation is very small for the Spherical Head Model. A constant bias of about 3% for the -2° position and less than 1% for the +88° position is noticed between experimental and numerical PF.

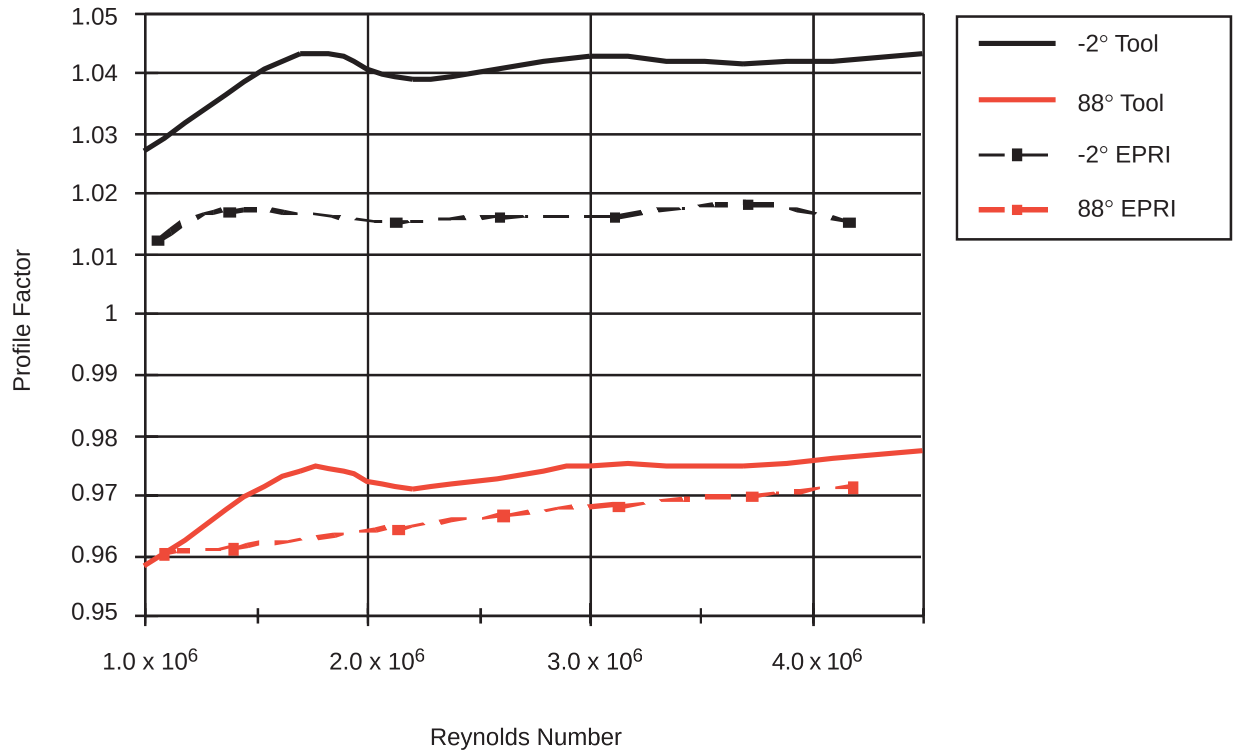

Figure 4-11
Variations of the Profile Factor with the Reynolds Number (Spherical Head Model) ("Tool" Stands for EdF Tool Results and "EPRI" Stands for EPRI Experimental Data)
SEE APPENDIX B FOR COLOR REPRESENTATION

The third comparison (see Figure 4-12) is the profile factor variations along of the 16" pipe axis. Again, it shows a good estimation of the profile factor value with a difference of 1.5%–2.5%.

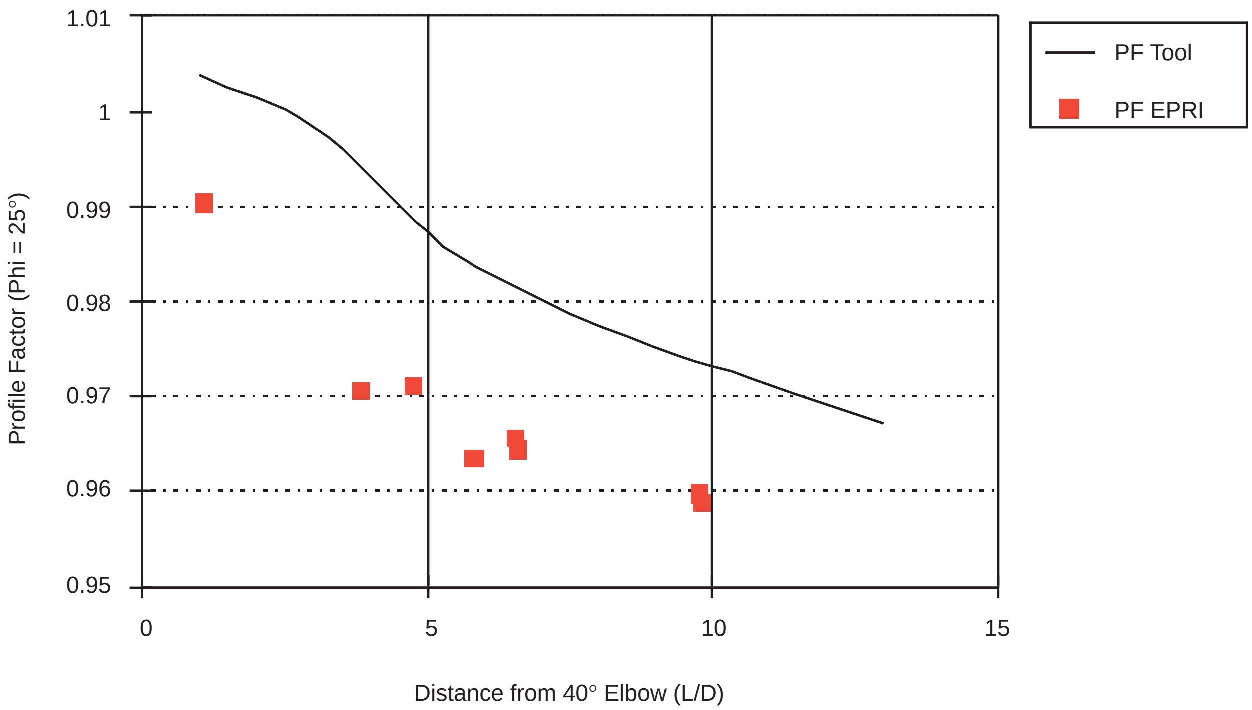

Figure 4-12
Variations of the Profile Factor with the Ultrasonic Middle Path Chord Position (Spherical Head Model) ("Tool" Stands for EdF Tool Results and "EPRI" Stands for EPRI Experimental Data)
See appendix B for color representation

Finally, the profile factor comparisons between the experiments and simulations were better than what was obtained with the Contraction Model because the latest ESTET version was used. In addition, the mesh was performed by a more efficient software.

5

MODEL SENSITIVITY AND DETERMINATION OF SIGNIFICANT VARIABLES

Overview

The objective of this analysis was to determine significant variables that affect modeling results. They can then be used to identify what parameters must be carefully evaluated for model use in plant-specific applications.

Mesh Independency

It is important to know the sensitivity of the computed results on mesh dimensions. Figure 5-1 shows the profile factor results obtained from a flow computed with two different grids for the Contraction Model. The first mesh is comprised of 194,145 nodes ($43 \times 43 \times 105$, I-, J-, K-planes). The second mesh is finer and consisted of 351,135 nodes ($51 \times 51 \times 135$, I-, J-, K-planes). At 1.6D, the maximum difference is 1%; whereas, there is no difference at 4.8D. This comparison shows that the first grid is well-sized and well-adapted for the computer runs.

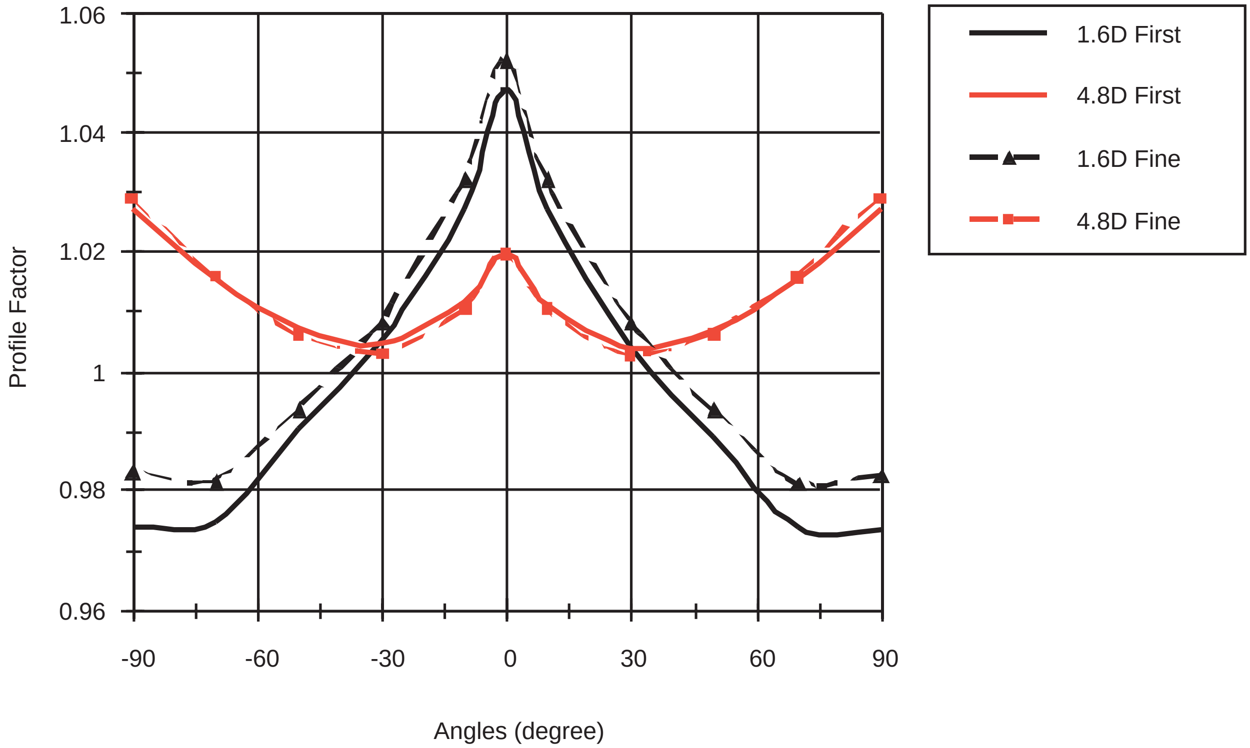

Figure 5-1
Comparison of Profile Factors Calculated from Two Different Contraction Model Meshes ("First" Is the Standard Mesh and "Fine" Is a Finer Mesh)
See appendix b for color representation

Reynolds Number

The Reynolds number sensitivity study presented in Figure 5-2 provides more information on the dependency between the profile factor and the Reynolds number of the fluid. A computer run was performed with a Reynolds number of 10^7 (inlet mean velocity equal to 102.3 in./s). The profile factor is slightly influenced by a variation of the Reynolds number at the 4.8D axial position: from 0% at 0° to a maximum slightly less than 2% at ±90° for Reynolds number, which varies from 10^6–10^7.

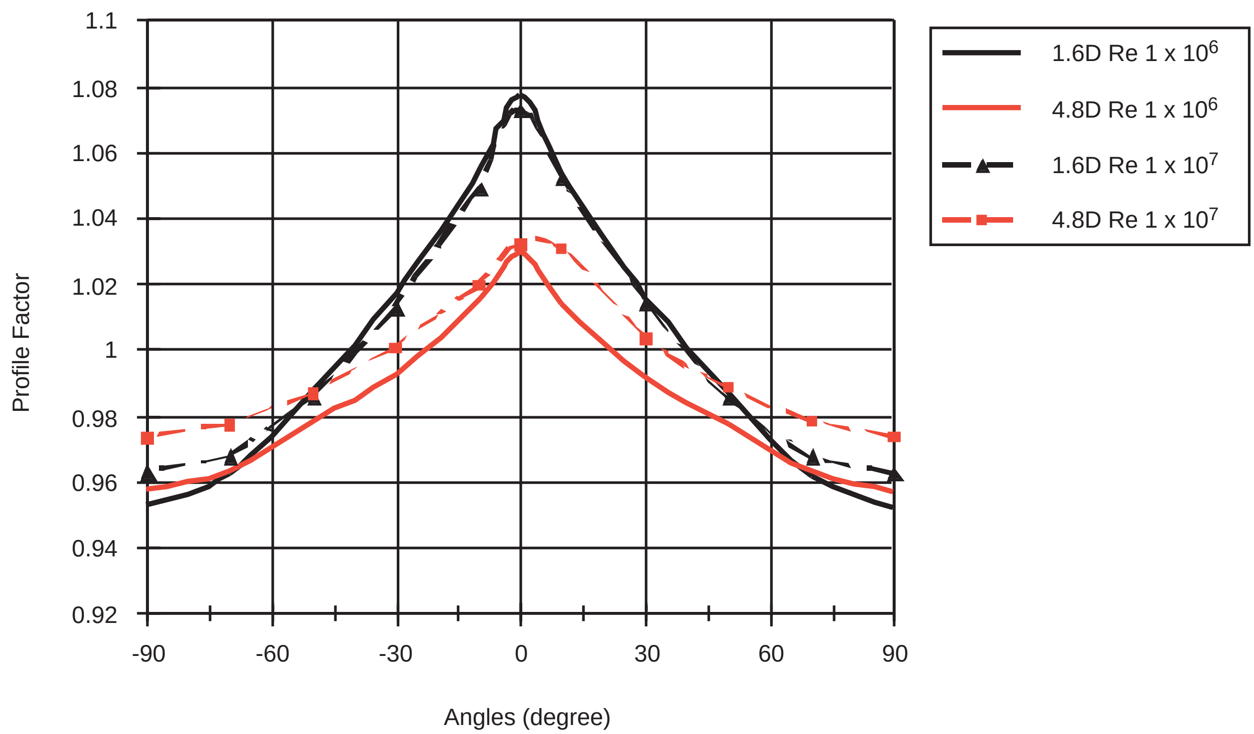

Figure 5-2
Comparison of Profile Factors Calculated for Two Different Reynolds Numbers (Spherical Head Model)
SEE APPENDIX B FOR COLOR REPRESENTATION

Inlet Velocity Conditions

For the Spherical Head Model, the influence of the inlet velocity conditions was examined. The two inlet axial velocity profile conditions chosen for the computer runs are plotted in Figure 5-3. In this case (see Figure 5-4), the profile factor is slightly influenced by the inlet velocity conditions; there is less than 1% difference between PF in the ±60° region. In fact, the inlet 24" pipe diameter is long enough to allow the velocity profile to stabilize before the inlet of the sphere. In the Spherical Head Model study, a flat inlet profile is sufficient and correct.

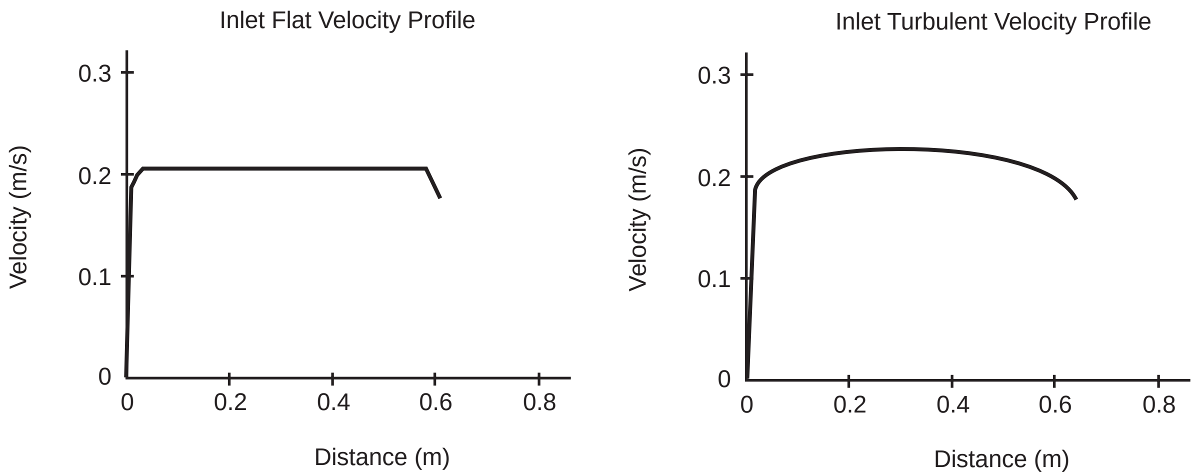

Figure 5-3
Flat and Turbulent Inlet Velocity Profiles (Spherical Head Model)

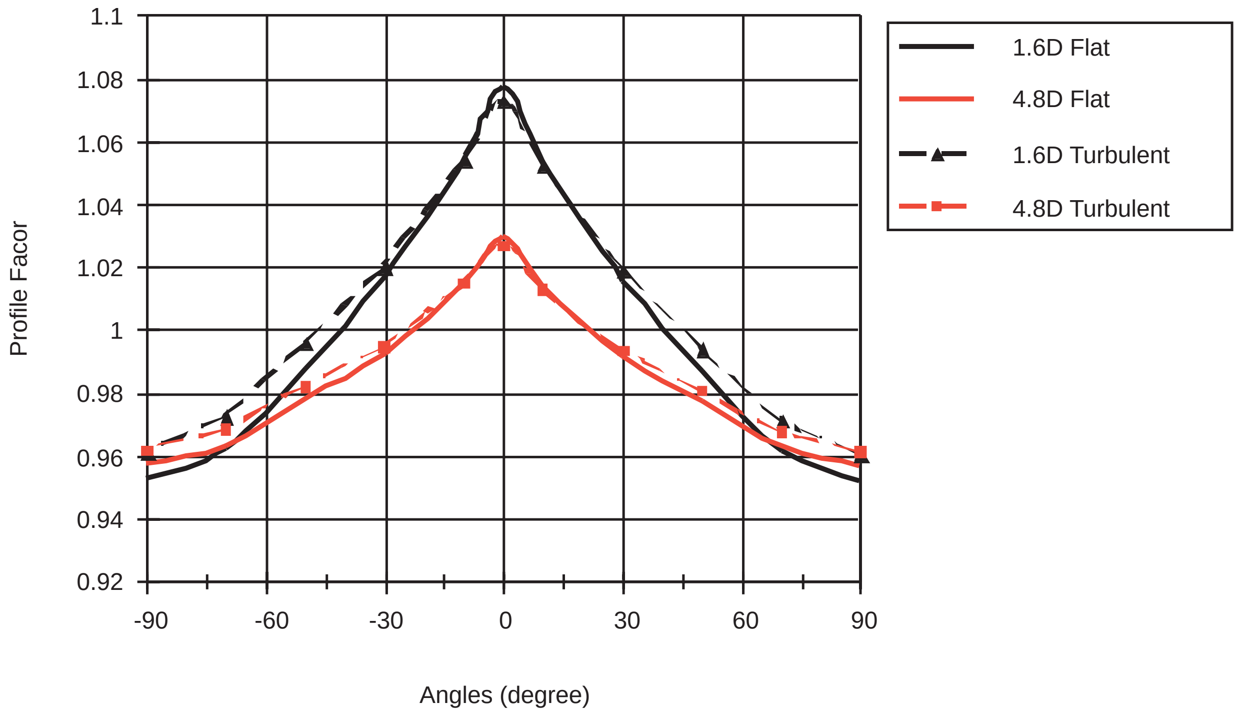

Figure 5-4
Comparison of Profile Factors Calculated from Two Different Inlet Velocity Profiles (Spherical Head Model)
SEE APPENDIX B FOR COLOR REPRESENTATION

Turbulence Model

In addition to the k-ε model, the RNG published model was tested for the Contraction Model. The profile factor results (see Figure 5-5) showed that the results from the RNG model are inferior to the k-ε model, especially for the 1.6D axial position (bias of up to 16%). On the basis of these results, it was decided not to perform a computer run of the Spherical Head Model with the RNG turbulence model.

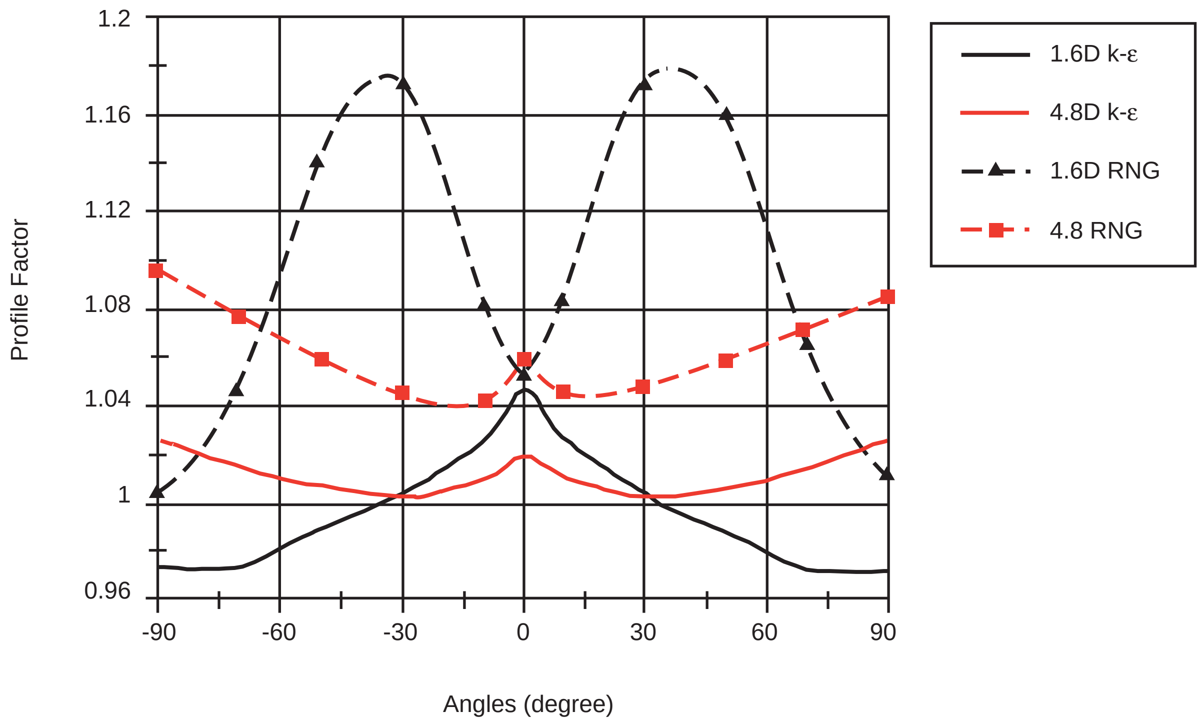

Figure 5-5
Comparison of Profile Factors Calculated from Two Different Turbulence Models (Contraction Model)
SEE APPENDIX B FOR COLOR REPRESENTATION

Physical Characteristics of the Fluid (Pressure and Temperature)

The last observation is on the influence of the temperature and pressure values on the flow simulation and, therefore, on the profile factor calculation. A fluid flow simulation, with the same Reynolds number at 300.15°K (80.6°F) for a pressure equal to the atmospheric pressure, is compared to the standard computation. These physical modifications give a constant difference of about 2% on the profile factor values.

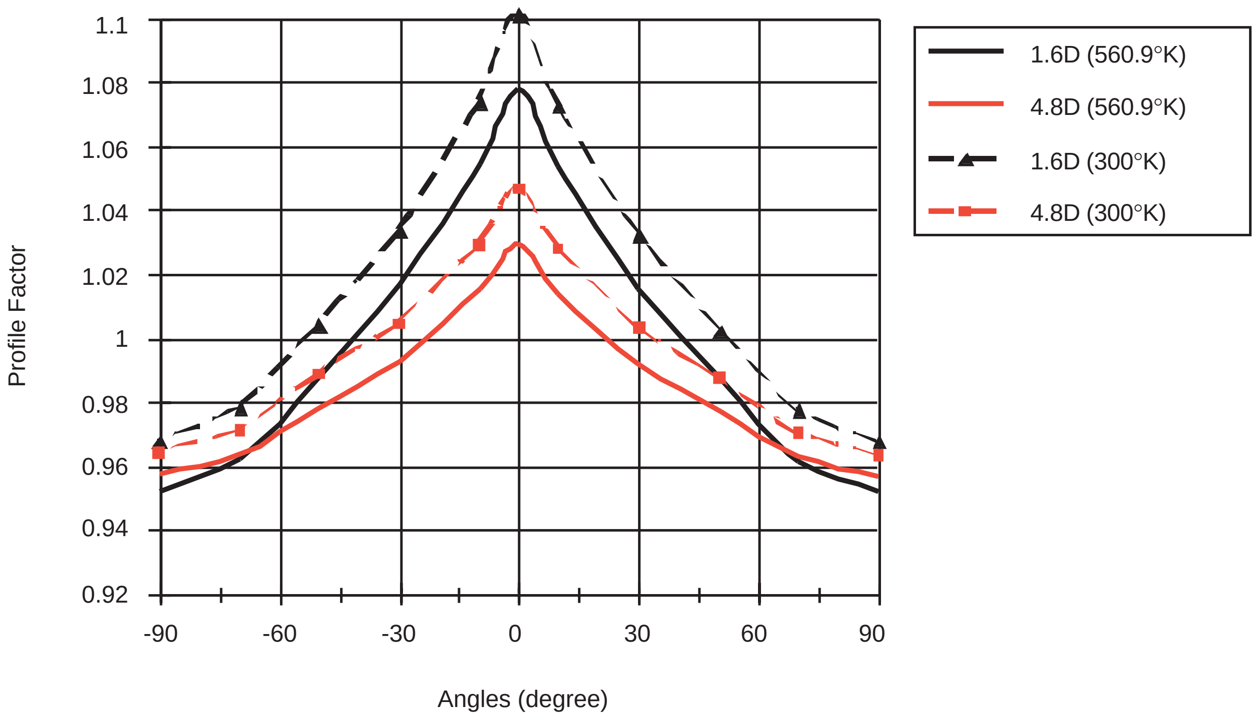

Figure 5-6
Comparison of Profile Factors Calculated from Different Physical Properties of the Fluid: 560.9°K (549.95°F) at 1.55 x 10^7 Pa (2.25 x 10^3 psia) and 300.15°K (80.6°F) at 1.013 x 10^5 Pa (1.47 x 10^1 psia) (Spherical Head Model)
SEE APPENDIX B FOR COLOR REPRESENTATION

6

SUMMARY AND CONCLUSIONS

Profile Factor Computations

This study consisted of modeling an isothermal stationary turbulent flow in two different pipe models: the Contraction Model and the Spherical Head Model, which were experimentally tested at the Alden Research Laboratory. For these two experimental installations, EPRI / ECD provided some profile factors obtained with a prototype ultrasonic PWR primary coolant flow measurement system.

The REME branch of EdF / DER developed a software tool to model the flow with the ESTET fluid dynamic code and to simulate the ultrasonic flow measurement instrumentation. This tool was used for the two EPRI models.

The profile factors obtained with the tool are overall in good agreement with the experimental data. For the Contraction Model, the typical difference between experimental and numerical profile factors is less than 3%; however, the maximum difference is as high as 10%. For the Spherical Head Model, the typical difference between experimental and numerical profile factors is less than 2%. The parametric studies of the profile factor with the Reynolds number and the ultrasonic middle path chord position show differences from 1%–3%. This bias is 1.5%–2.5% for the variations of the profile factor with the axial position. The accuracy of the experimental profile factor is ±0.65%.

The evolution of the ESTET code between the development of the Contraction Model and the Spherical Head Model could explain why the results are more accurate for the latter configuration.

Model Sensitivity

This study provides some information on the profile factor dependencies.

The mesh independency study shows that an increase of 80% of the grid node number might lead to a maximum change in the profile factors of 1% at 1.6D and no effect to the profile factor at 4.8D. The grid that was used for all computer runs proved to be well adapted.

When the flow is turbulent, the profile factor is slightly influenced by the fluid Reynolds number; a maximum bias of 2% can be reached for particular angular and axial positions of the flow meter when the Reynolds number varies from 10^6–10^7.

On the other hand, the profile factor can vary with the temperature and pressure for a constant Reynolds number; a bias of 2% was found between the PF calculated at 560°K (548.33°F), 1.55 x 10^7 Pa (2.25 x 10^3 psia) and 300°K (80.33°F), 1 x 10^5 Pa (1.45 x 10^1 psia).

The choice of the turbulence model for the modeling is important. This choice depends on the CFD code, the fluid flow structure, and the expected accuracy of the results. The k-ε turbulent model gives a good prediction of the fluid behavior, if the flow does not swirl (which was the case of the ARL models). On the contrary, the RNG model seems not to be well adapted.

The last information is about the inlet velocity profile. If the straight inlet pipe is long enough, the inlet velocity profile conditions are of negligible importance; a bias of less than 1% was found for some angles.

Conclusions

The profile factors obtained with the tool are overall in good agreement with the experimental data. Except for some specific angular and axial positions of the flow profile meter, the typical difference between experimental and numerical profile factors is 2% or 3%, according to the model.

The influence of the significant factors in determining the flow profile factor has been quantified. If the straight inlet pipe is long enough, parametric studies showed that the inlet velocity profile is of negligible influence. When the flow is turbulent, the profile factor is slightly influenced by the fluid Reynolds number: a maximum bias of 2% was found when the Reynolds number varies from 10^6–10^7. However, the profile factor can vary with temperature and pressure for a constant Reynolds number: a bias of 2% was determined between profile factors calculated at 560°K (548.33°F), 1.55 x 10^7 Pascals (Pa) (2.25 x 10^3 psia) and 300°K (80.33°F), 1 x 10^5 Pa (1.45 x 10^1 psia). The choice of the turbulence model is important. The k-ε turbulent model predicted the fluid behavior accurately, likely due to a lack of swirling in the flow.

The obtained results show that the modeling approach for the profile factor determination is feasible and could be a substitute to the experimental approach. Some significant variables in determining the flow profile factor have been identified and their influence quantified. The determined values could be used as an indication for future studies, but it is important to consider each case as a specific study. In this context, the objective of generically calculating profile factors is far from being reached. A way to get closer to it would be to carry out an exhaustive study of geometrical singularities present in power plants with parametric studies on all significant plant conditions.

Finally, the model user must be properly trained in the use of this tool. The user must know when the modeling solutions converge, because a small variation in the velocity profile could introduce a profile factor calculation error of several percentage points. The mesh domain also plays an important part in the accuracy of the final result and has to be reviewed carefully.

Recommendations for Future Work

To complete this study, three short-term improvements in the profile factor computations are proposed.

1. Contraction Model

   The difference between the experimental and numerical results for the 4.8D axial position of the meter might be corrected by carrying out the mesh with the ICEM software. In addition, better results can be obtained by re-running the computation with the last ESTET version (3.2.2) that was used for the Spherical Head Model, which proved to be superior.

2. Turbulence Model

   To complete the turbulence model study, it is recommended that the computer runs be performed with the Reynolds stress turbulence model that is best adapted for flows with swirl, which is frequent in real industrial flows.

3. Influence of the Transverse Fluid Velocity

Finally, as the EdF tool is dedicated to standard industrial ultrasonic flowmeters, it takes into account the transverse fluid velocity influence in the profile factor calculation. The EPRI RCMS prototype corrects this influence in the flow meter by taking cross-path measurements that cancel any transverse fluid velocity contribution [3] (Paragraph 2). Even though the modeling results show that the transverse velocity’s contribution to the profile factor correction is small, it is recommended that additional computer runs be conducted with removal of the transverse velocity contributions.

7

REFERENCES

1. Memorandum of Understanding between EPRI/NPG and EdF/DER, “Modeling Pipe Flow for Ultrasonic Temperature and Flow Measurement Instrumentation,” April 1997.
2. EdF Technical Report, “Mesure du débit des liquides par débitmètres accrochables à ultrasons,” ref. HP-12/91.26, October 1991.
3. EPRI Technical Report, “Design, Installation and Testing of Prototype Ultrasonic PWR Primary Coolant Temperature/Flow Measurement System (RCMS),” ref. TR-106821, Vol. 2, December 1996.
4. EdF Technical Report, “Système ESTET-ASTRID. Manuel théorique. Version 3.2,” ref. HE-44/95, 1995.

A

PROFILE FACTOR RESULTS

This appendix groups together the profile factor simulations for all the study cases. Caution, the digit number uses the French convention: the decimal value is separated by a comma, not by a point.

Contraction Model

Table A-1
Data for Figure 3-8

Angles	1.6D Tool	4.8D Tool
90	0,9732	1,0268
70	0,9735	1,0152
50	0,989	1,0068
30	1,0041	1,0038
10	1,0271	1,0111
0	1,047	1,0197
-10	1,0271	1,0115
-30	1,0051	1,0045
-50	0,9902	1,0072
-70	0,9747	1,0154
-90	0,9738	1,0269

Table A-2
Data for Figure 3-9

Nb Reynolds	-2° Tool	88° Tool
1,00E+06	1,0437	0,9725
1,50E+06	1,0445	0,9741
2,50E+06	1,0459	0,9779
3,00E+06	1,0464	0,9786
4,00E+06	1,0456	0,9796
4,50E+06		

Table A-3
Data for Figure 5-1

Angles	1.6D first	4.8D first
90	0,9732	1,0268
70	0,9735	1,0152
50	0,989	1,0068
30	1,0041	1,0038
10	1,0271	1,0111
0	1,047	1,0197
-10	1,0271	1,0115
-30	1,0051	1,0045
-50	0,9902	1,0072
-70	0,9747	1,0154
-90	0,9738	1,0269

1.6 Dfine	4.8D fine
0,9825	1,0287
0,981	1,01566
0,9936	1,0061
1,0081	1,0025
1,0321	1,0103
1,052	1,0195
1,032	1,0104
1,0082	1,0027
0,9935	1,0062
0,9813	1,0158
0,9831	1,0289

Table A-4
Data for Figure 5-5

1.6D k-eps	4.8D k-eps
0,9732	1,0268
0,9735	1,0152
0,989	1,0068
1,0041	1,0038
1,0271	1,0111
1,047	1,0197
1,0271	1,0115
1,0051	1,0045
0,9902	1,0072
0,9747	1,0154
0,9738	1,0269

1.6D rng	4.8D rng
1,0094	1,08488
1,06219	1,0705
1,15862	1,05782
1,17316	1,04616
1,0825	1,04442
1,05395	1,0588
1,0831	1,04092
1,17106	1,04454
1,142	1,05964
1,04678	1,07682
1,0022	1,09486

Spherical Head Model

Table A-5
Data for Figure 4-10

Angles	1.6D Tool	4.8D Tool
90	0,95202	0,95703
70	0,96144	0,96282
50	0,98664	0,97703
30	1,01537	0,99156
10	1,05353	1,01357
0	1,07761	1,02912
-10	1,0548	1,01534
-30	1,01654	0,9927
-50	0,98751	0,978
-70	0,96198	0,96349
-90	0,95242	0,95739

Table A-6
Data for Figure 4-11

Nb Reynolds	-2° Tool	88° Tool
1,00E+06	1,027	0,958
1,70E+06	1,0429	0,974
2,20E+06	1,039	0,971
3,00E+06	1,0426	0,975
3,70E+06	1,0415	0,975
4,50E+06	1,043	0,977

Table A-7
Data for Figure 4-12

L/D	PF Tool
1	1,0038
3	0,99846
5	0,98724
6	0,98322
8	0,97754
10	0,97306
13	0,96721

Table A-8
Data for Figure 5-2

Angles	1.6D Re 1E6	4.8D Re 1E6	1.6D Re 1E7	4.8D Re 1E7
90	0,95202	0,95703	0,96242	0,97342
70	0,96144	0,96282	0,96757	0,97811
50	0,98664	0,97703	0,98561	0,98829
30	1,01537	0,99156	1,01403	1,00296
10	1,05353	1,01357	1,05193	1,0306
0	1,07761	1,02912	1,07247	1,03189
-10	1,0548	1,01534	1,04895	1,0192
-30	1,01654	0,9927	1,01232	1,00038
-50	0,98751	0,978	0,98529	0,98651
-70	0,96198	0,96349	0,96781	0,97711
-90	0,95242	0,95739	0,96255	0,97307

Table A-9
Data for Figure 5-4

Angles	1.6D flat	4.8D flat	1.6D turbulent	4.8D turbulent
90	0,95202	0,95703	0,96064	0,96097
70	0,96144	0,96282	0,97115	0,96745
50	0,98664	0,97703	0,9939	0,98038
30	1,01537	0,99156	1,01846	0,99321
10	1,05353	1,01357	1,05186	1,01247
0	1,07761	1,02912	1,07287	1,0264
-10	1,0548	1,01534	1,05366	1,01436
-30	1,01654	0,9927	1,02005	0,9945
-50	0,98751	0,978	0,99521	0,9815
-70	0,96198	0,96349	0,97204	0,9683
-90	0,95242	0,95739	0,96114	0,96152

Table A-10
Data for Figure 5-6

Angles	1.6D (560.9 K)	4.8D (560.9 K)	1.6D (300 K)	4.8D (300 K)
90	0,95202	0,95703	0,96722	0,96344
70	0,96144	0,96282	0,97731	0,97045
50	0,98664	0,97703	1,00199	0,9877
30	1,01537	0,99156	1,03228	1,00329
10	1,05353	1,01357	1,07233	1,02808
0	1,07761	1,02912	1,10089	1,04668
-10	1,0548	1,01534	1,07356	1,02934
-30	1,01654	0,9927	1,03332	1,00415
-50	0,98751	0,978	1,00385	0,98846
-70	0,96198	0,96349	0,97786	0,97101
-90	0,95242	0,95739	0,96746	0,96381

B

COLOR IMAGES OF SELECTED FIGURES

Section 2 Figure

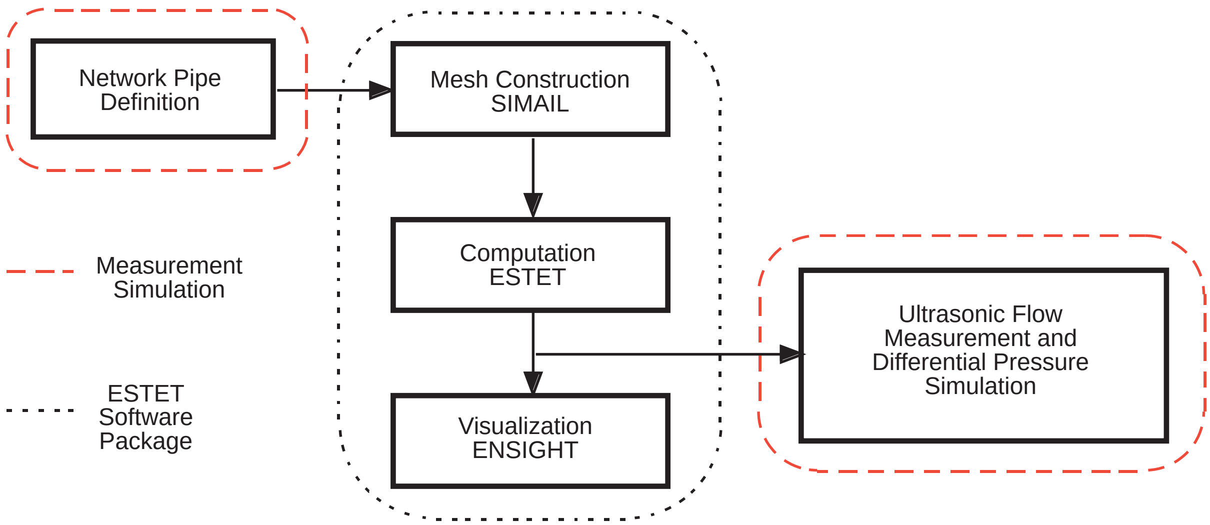

Figure B–2-1
EdF/DER Tool for Flow Rate Measurement Simulation

Section 3 Figures

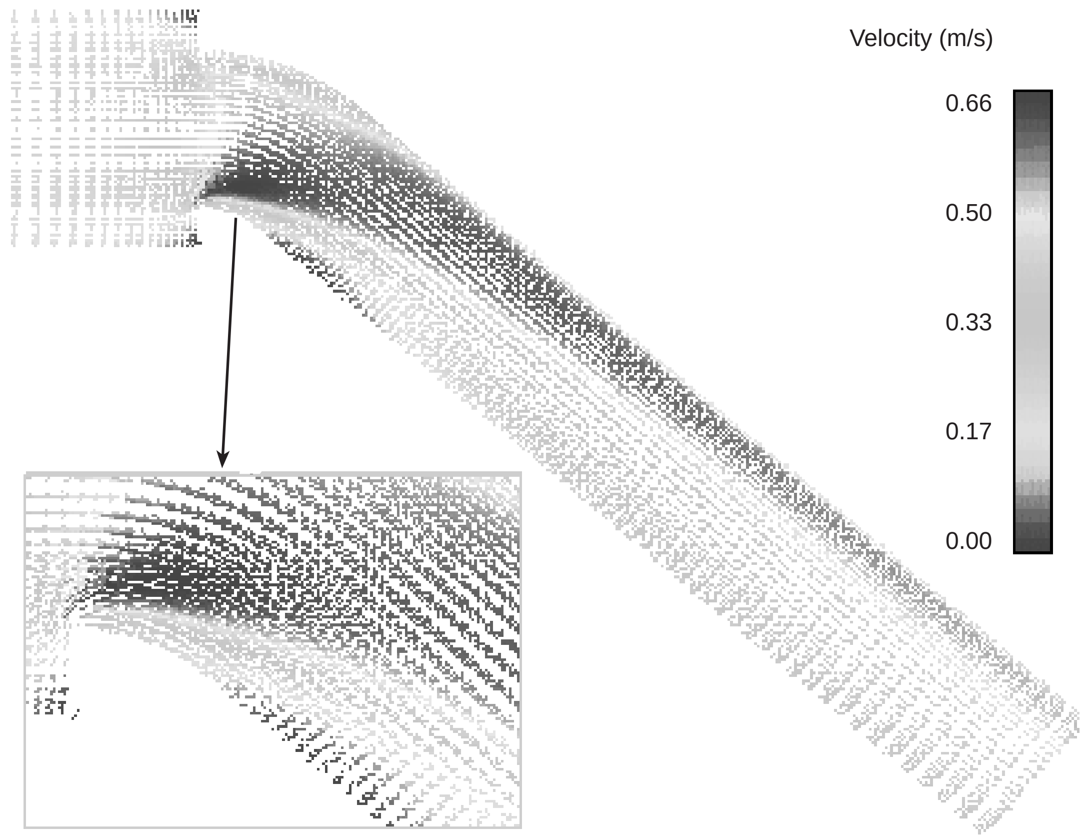

Figure B–3-3
Longitudinal Velocity Profile in the Middle Vertical Plan (Contraction Model)

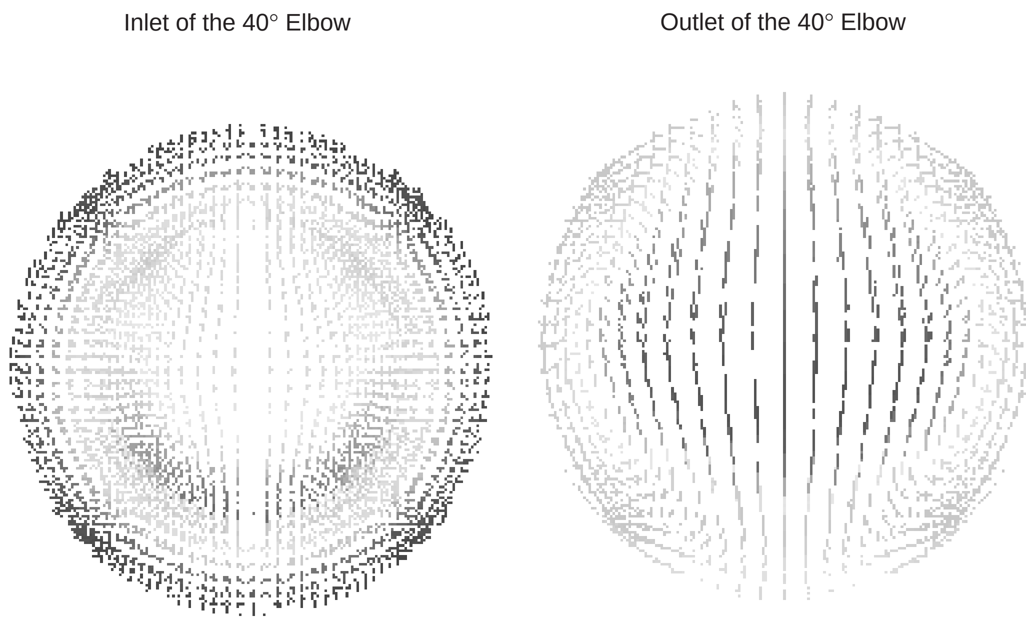

Figure B–3-4
Tangential Velocity Profiles in the Pipe Section at the Inlet and Outlet of the 40° Elbow (Contraction Model)

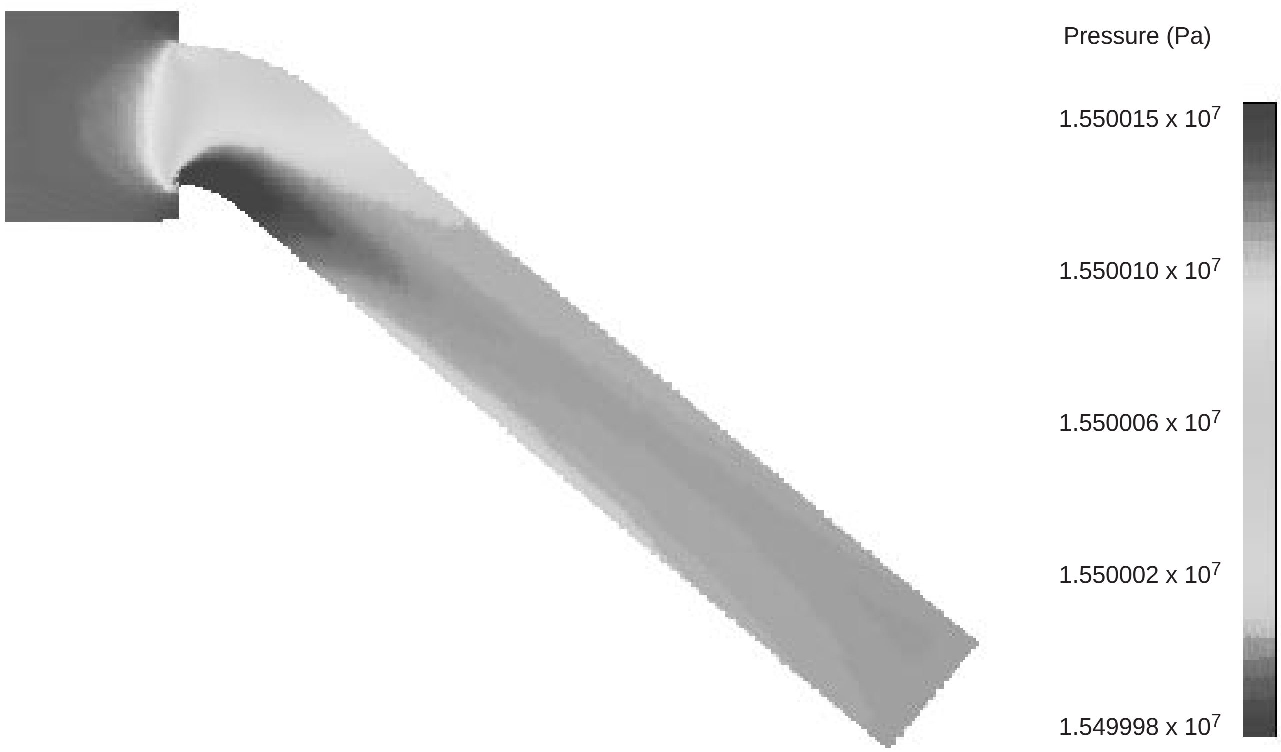

Figure B–3-5
Pressure Field in the Middle Vertical Plan (Contraction Model)

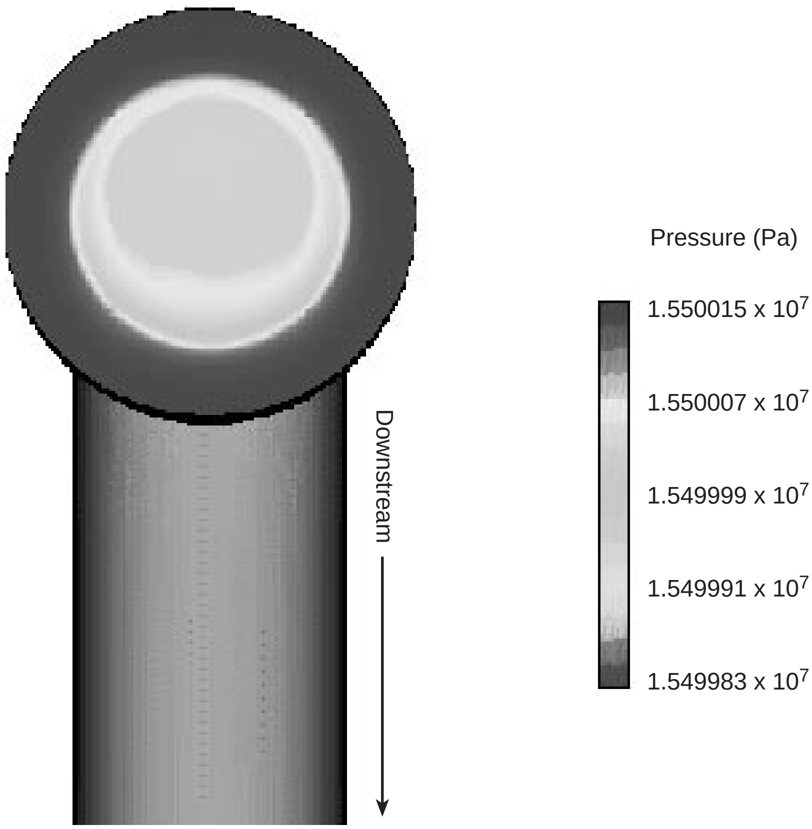

Figure B–3-6
Pressure in the Pipe Section at the Inlet of the 40° Elbow (Contraction Model)

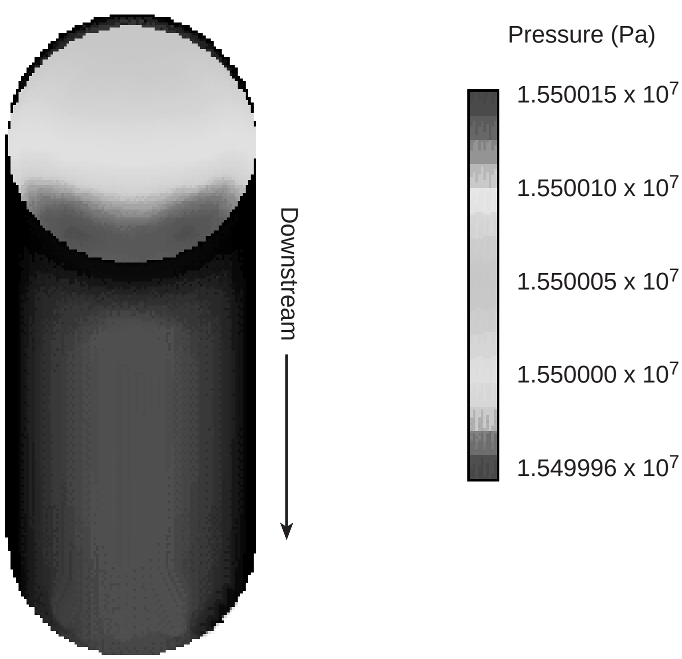

Figure B–3-7
Pressure in the Pipe Section at the Outlet of the 40° Elbow (Contraction Model)

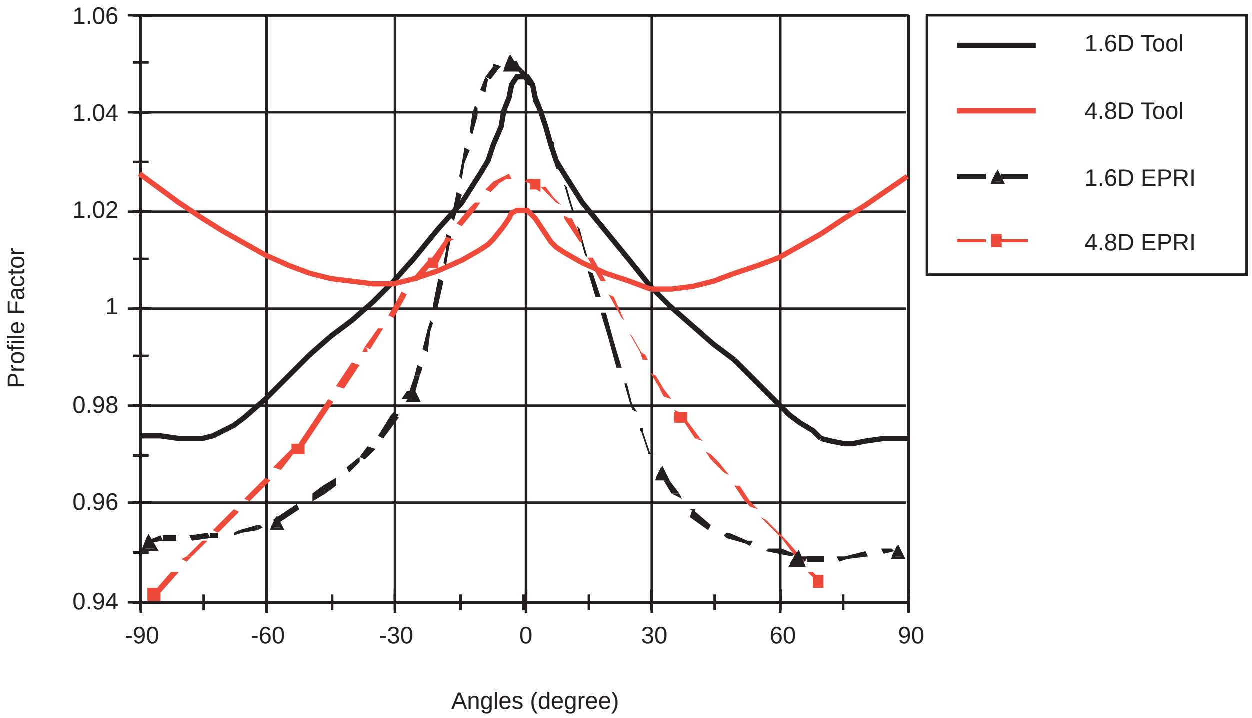

Figure B–3-8
Variations of the Profile Factor with the Angle (Contraction Model)
("Tool" Stands for EdF Tool Results and "EPRI" Stands for EPRI Experimental Data)

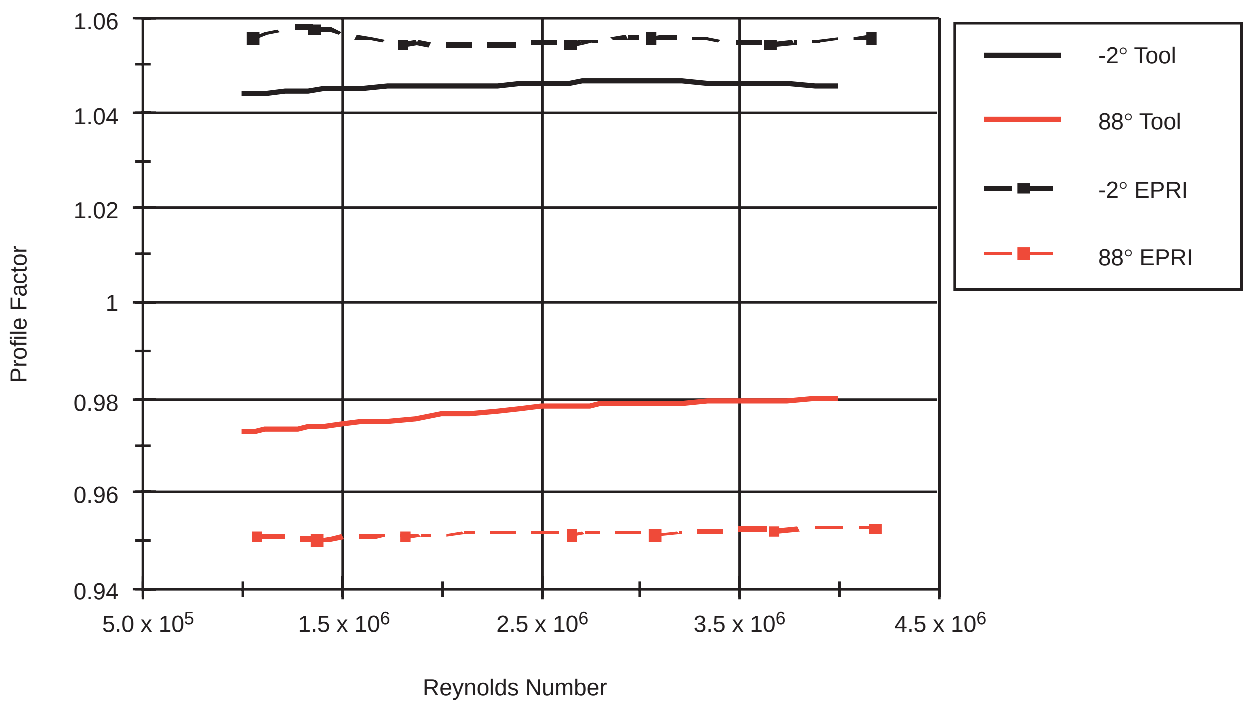

FigureB–3-9
Variations of the Profile Factor with the Reynolds Number (Contraction Model)

Section 4 Figures

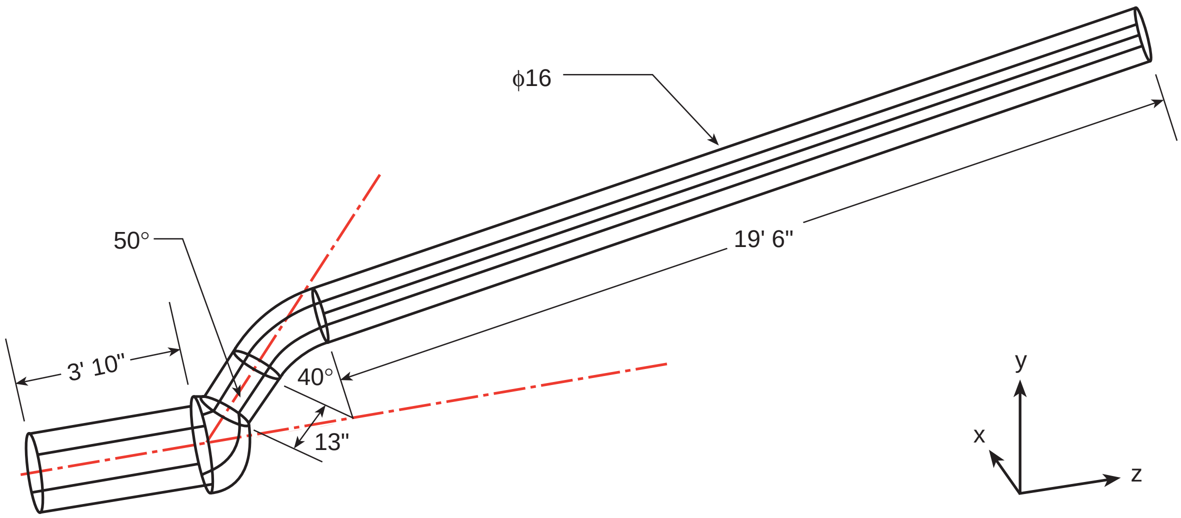

Figure B–4-1
Geometry of the Spherical Head Model

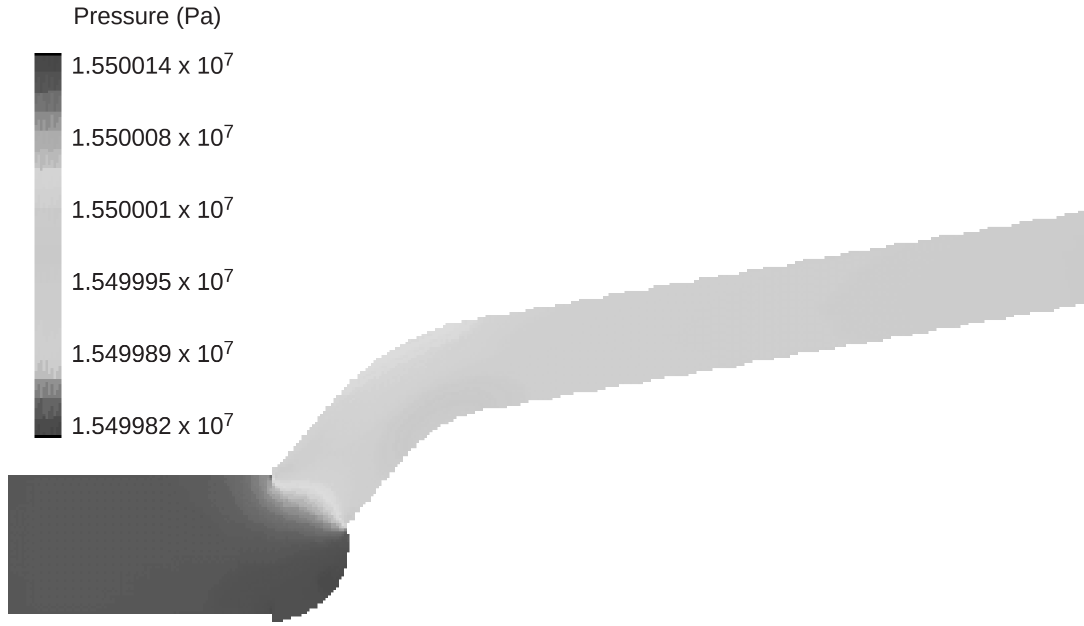

Figure B–4-5
Pressure Field in the Middle Vertical Plan (Spherical Head Model)

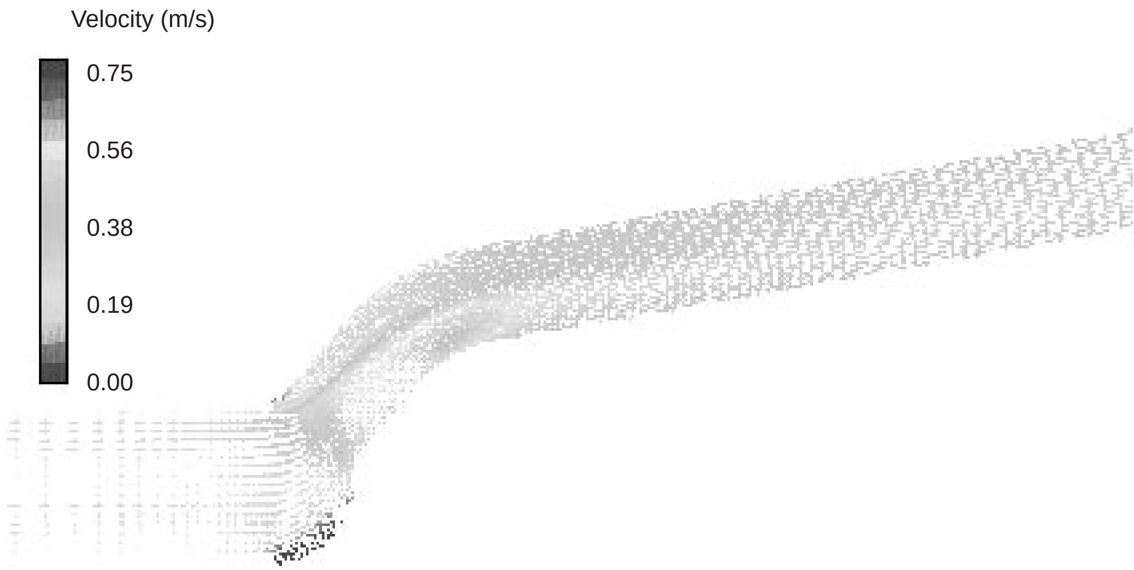

Figure B–4-6
Velocity in the Middle Vertical Plan (Spherical Head Model)

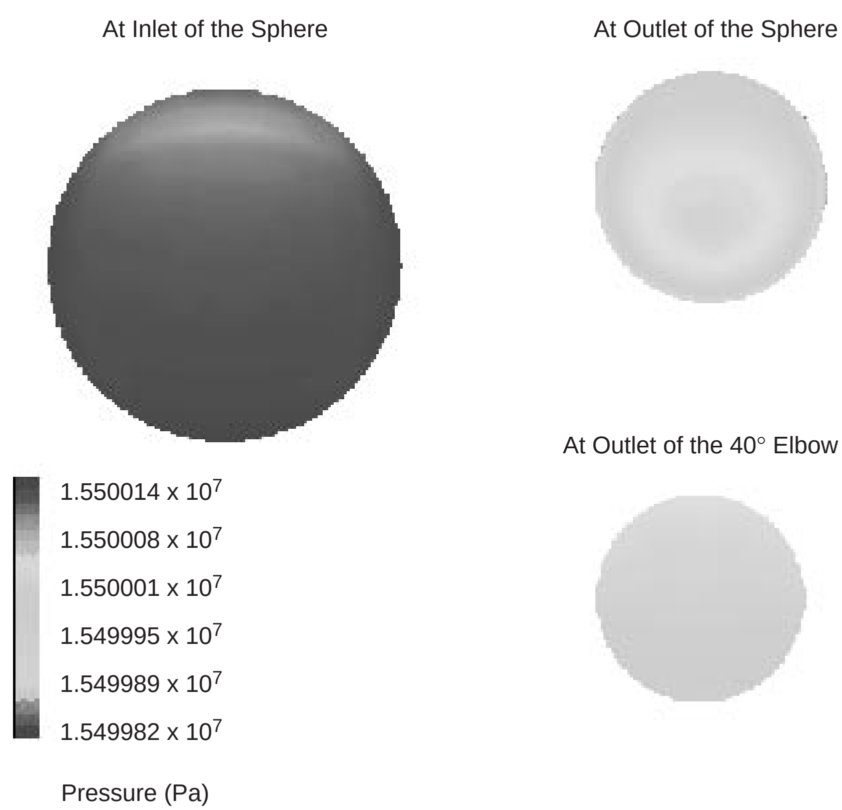

Figure B–4-7
Pressure Field in Pipe Sections Perpendicular to the Flow (Spherical Head Model)

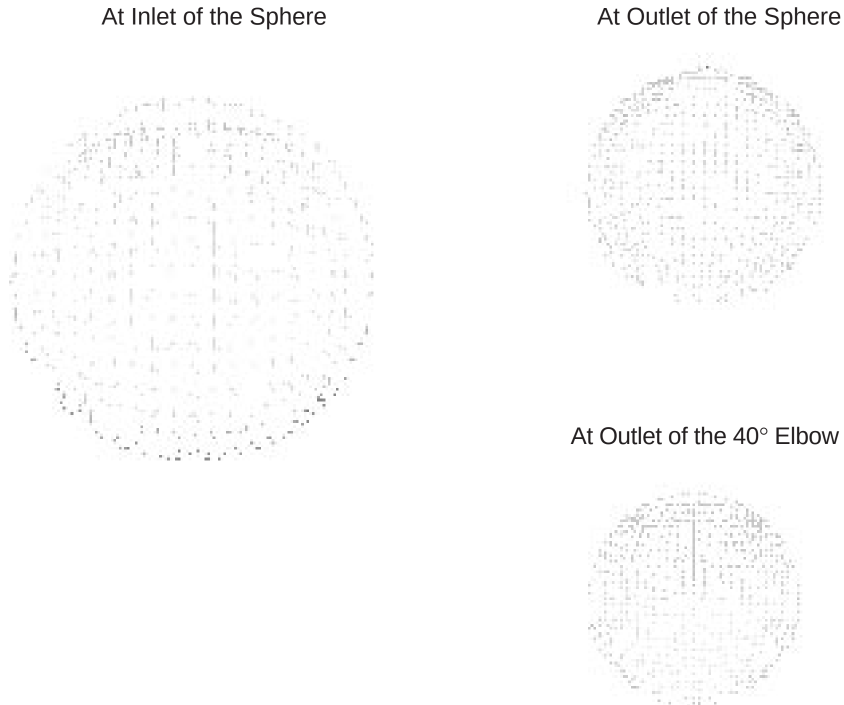

Figure B–4-8
Tangential Velocity in Pipe Sections Perpendicular to the Flow (Spherical Head Model)

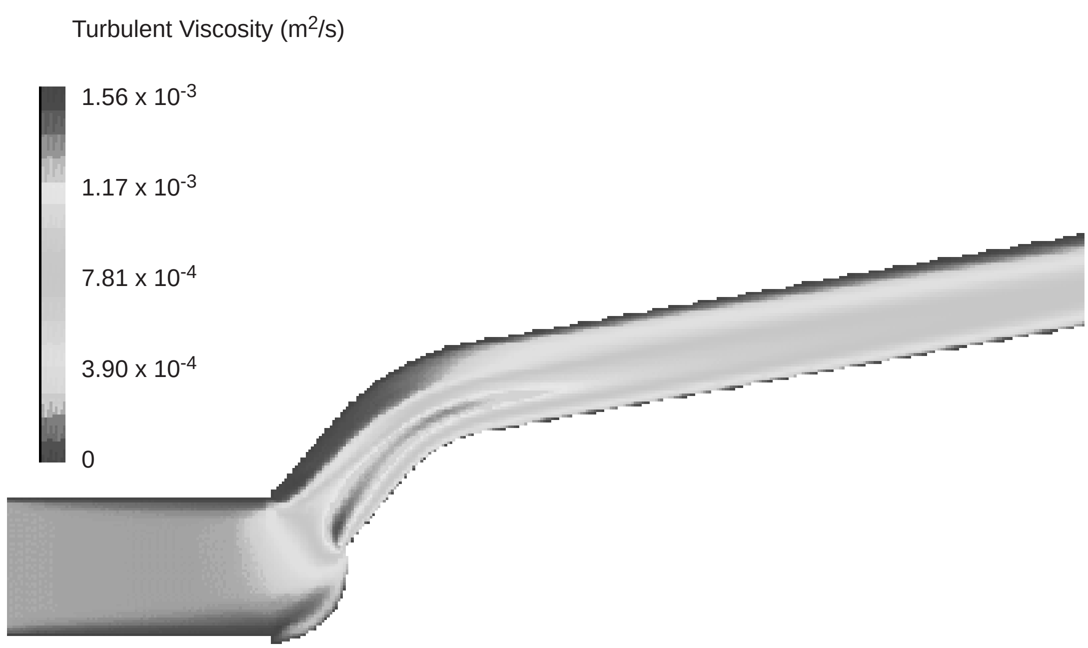

Figure B–4-9
Turbulent Viscosity in the Middle Vertical Plan (Spherical Head Model)

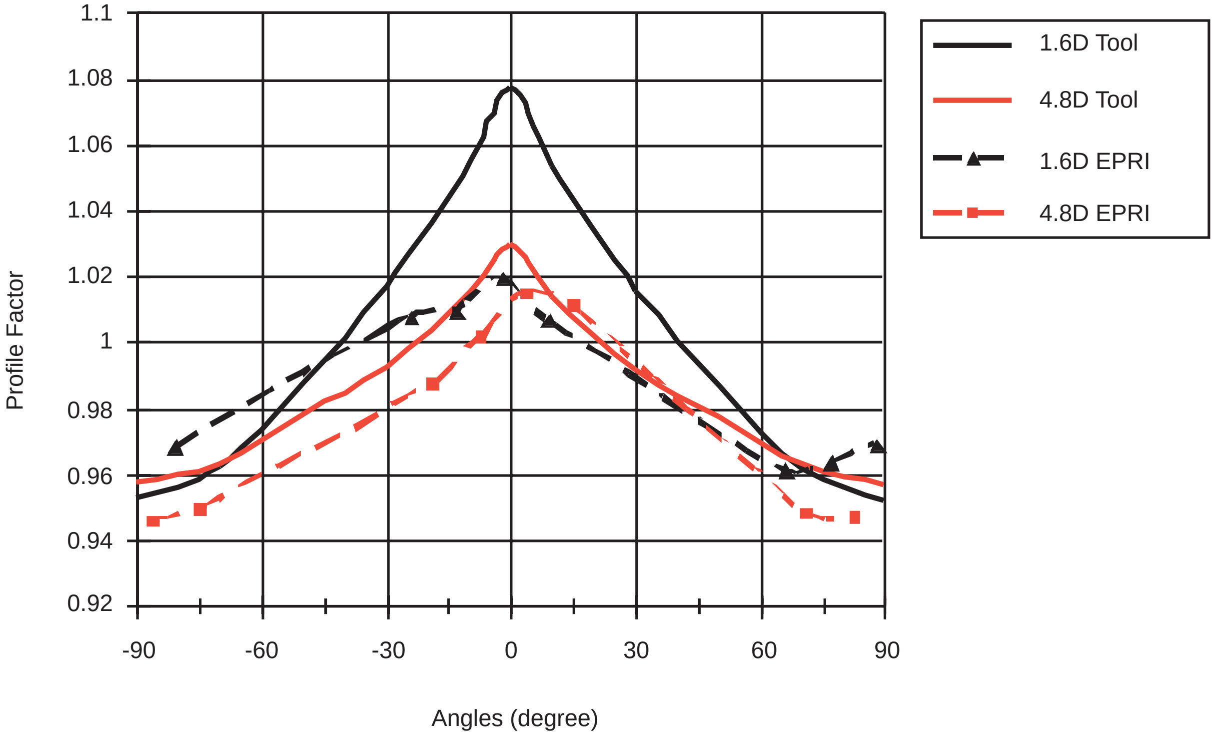

Figure B–4-10
Variations of the Profile Factor with the Angle (Spherical Head Model)
(“Tool” Stands for EdF Tool Results and “EPRI” Stands for EPRI Experimental Data)

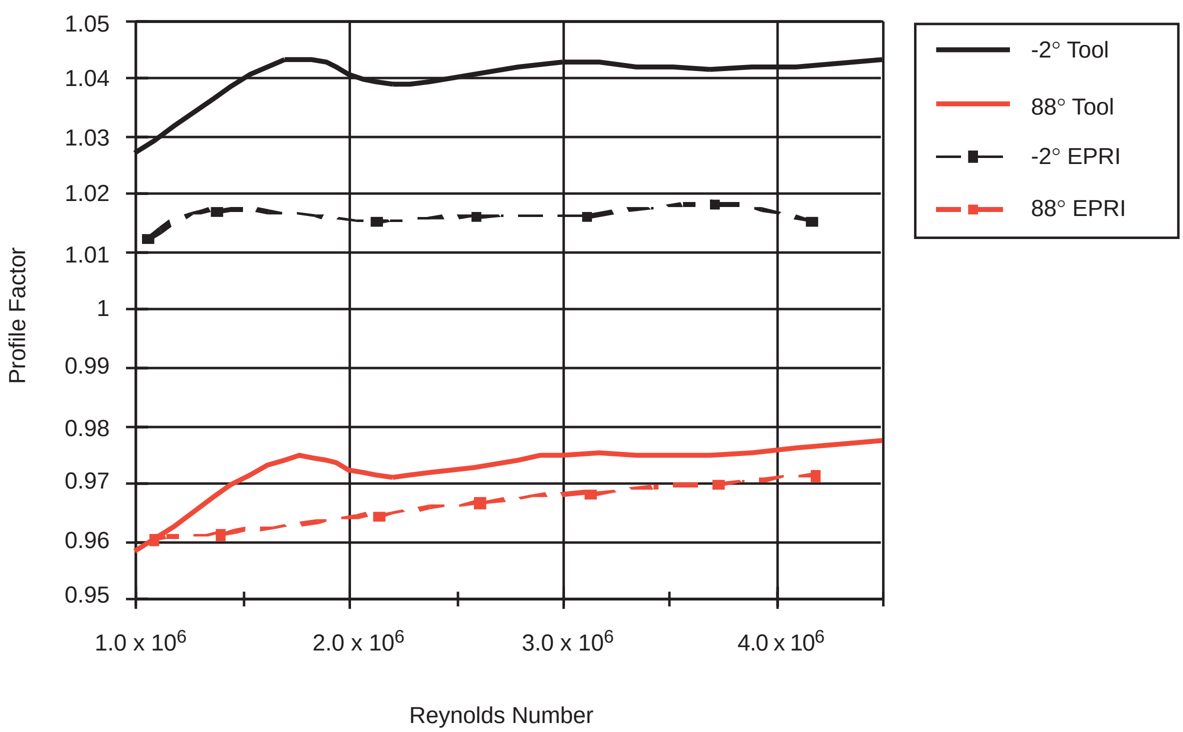

Figure B–4-11
Variations of the Profile Factor with the Reynolds Number (Spherical Head Model)
(“Tool” Stands for EdF Tool Results and “EPRI” Stands for EPRI Experimental Data)

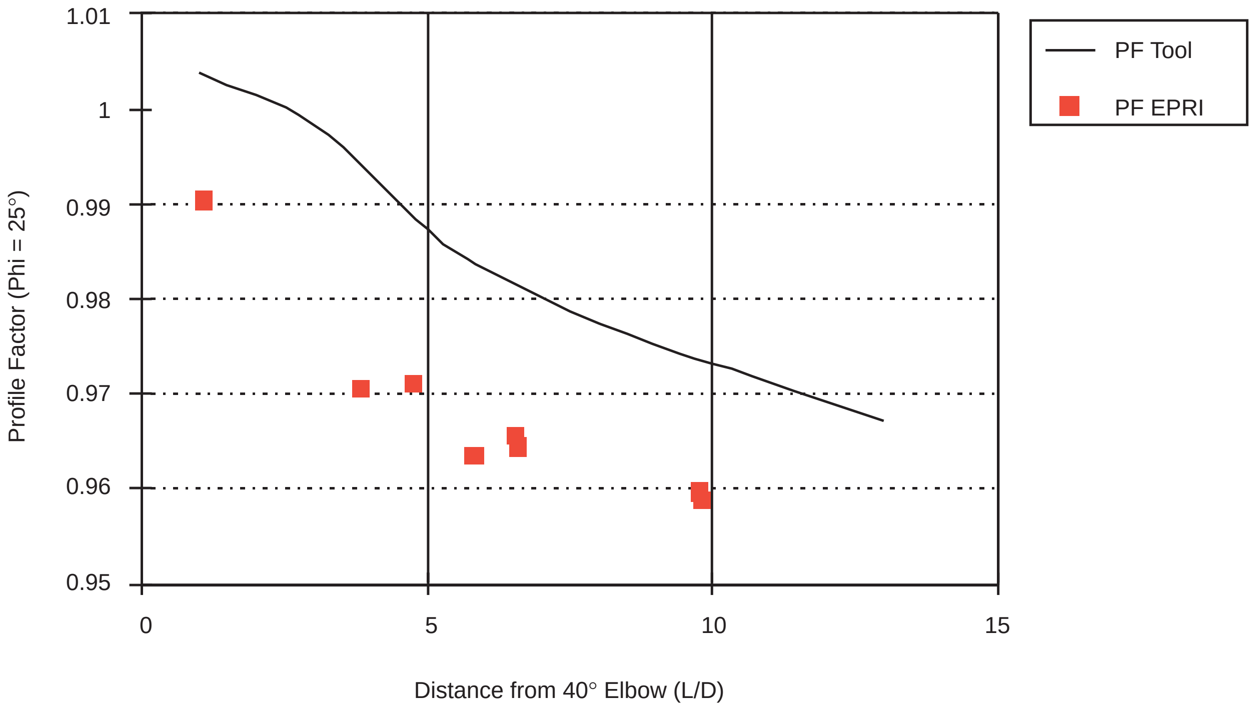

Figure B–4-12
Variations of the Profile Factor with the Ultrasonic Middle Path Chord Position (Spherical Head Model) ("Tool" Stands for EdF Tool Results and "EPRI" Stands for EPRI Experimental Data)

Section 5 Figures

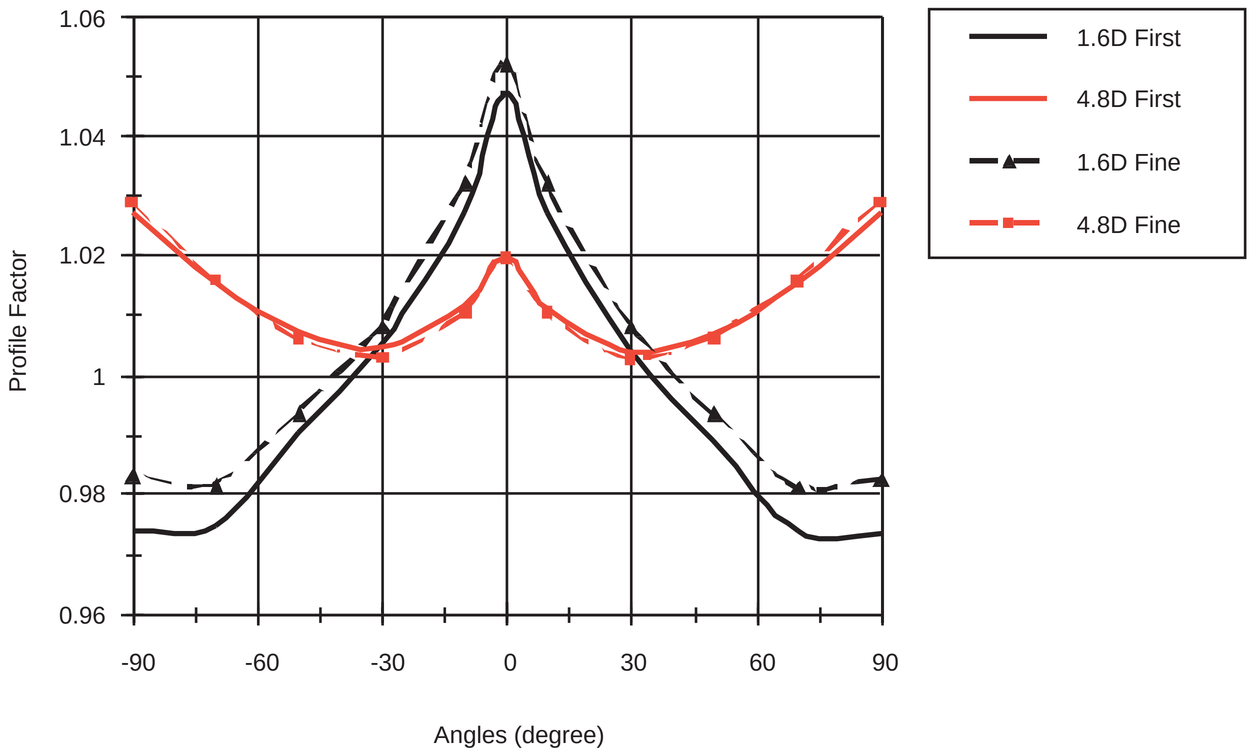

Figure B–5-1
Comparison of Profile Factors Calculated from Two Different Contraction Model Meshes ("First" Is the Standard Mesh and "Fine" Is a Finer Mesh)

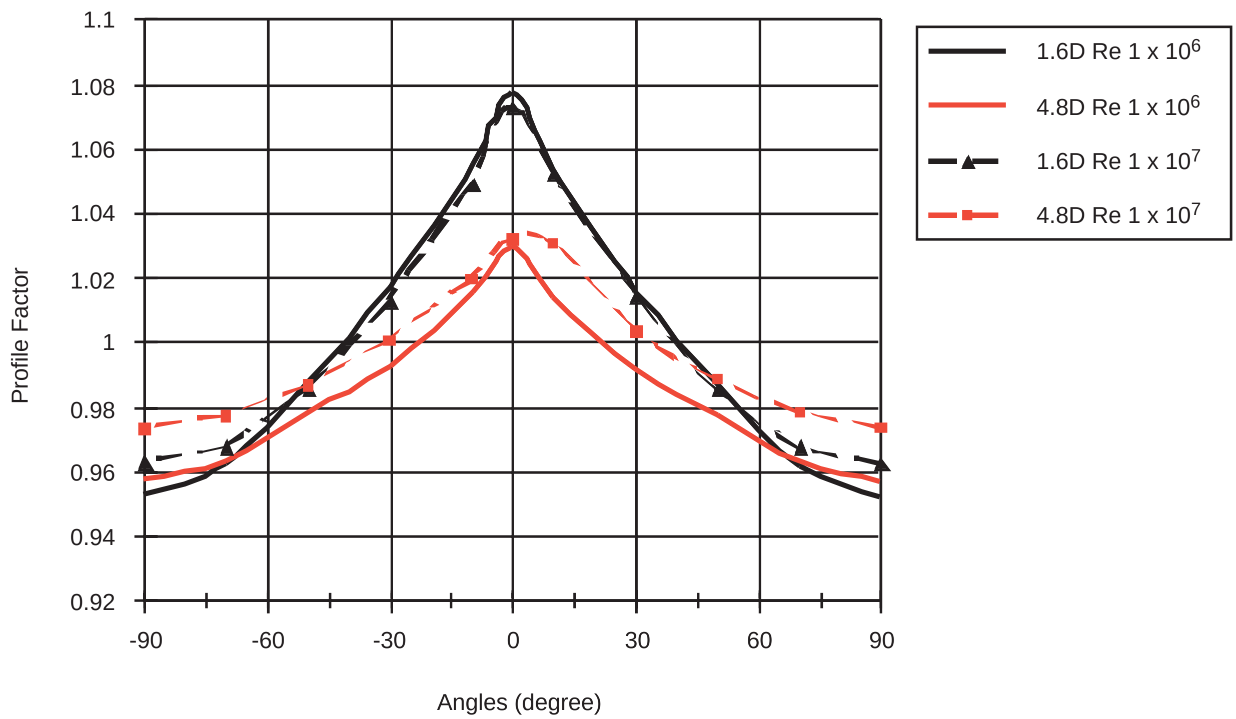

Figure B–5-2
Comparison of Profile Factors Calculated for Two Different Reynolds Numbers (Spherical Head Model)

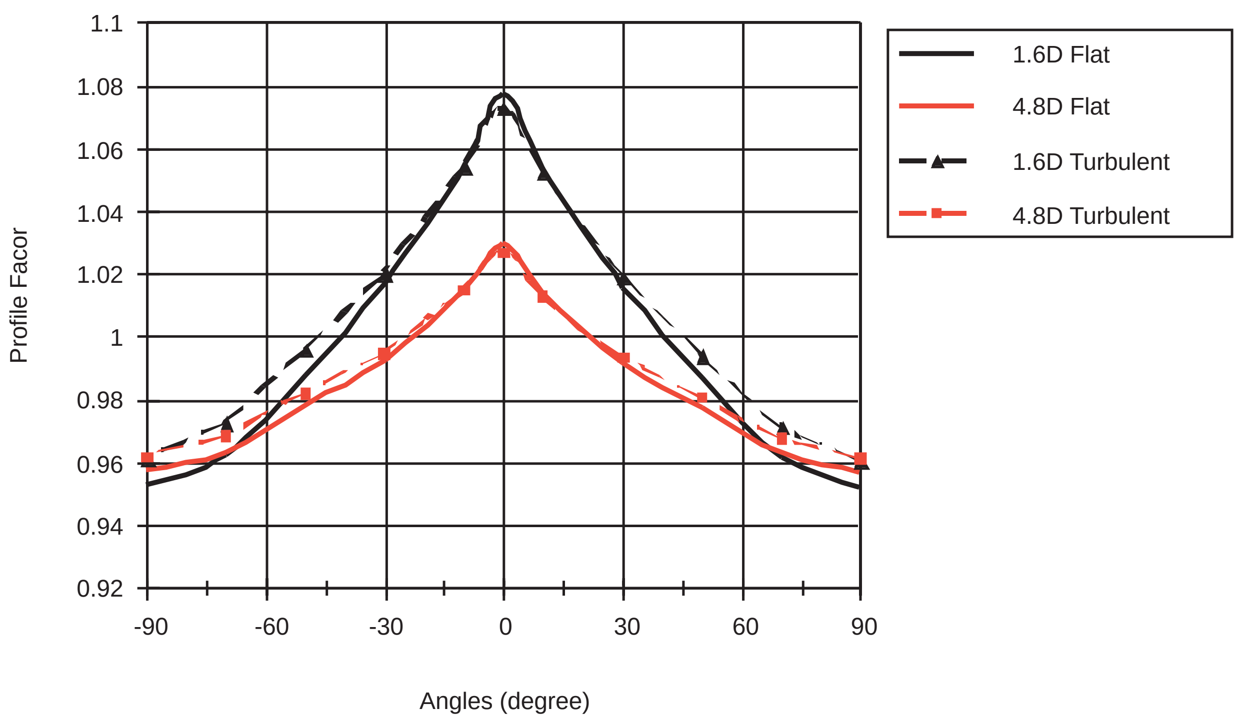

Figure B–5-4
Comparison of Profile Factors Calculated from Two Different Inlet Velocity Profiles (Spherical Head Model)

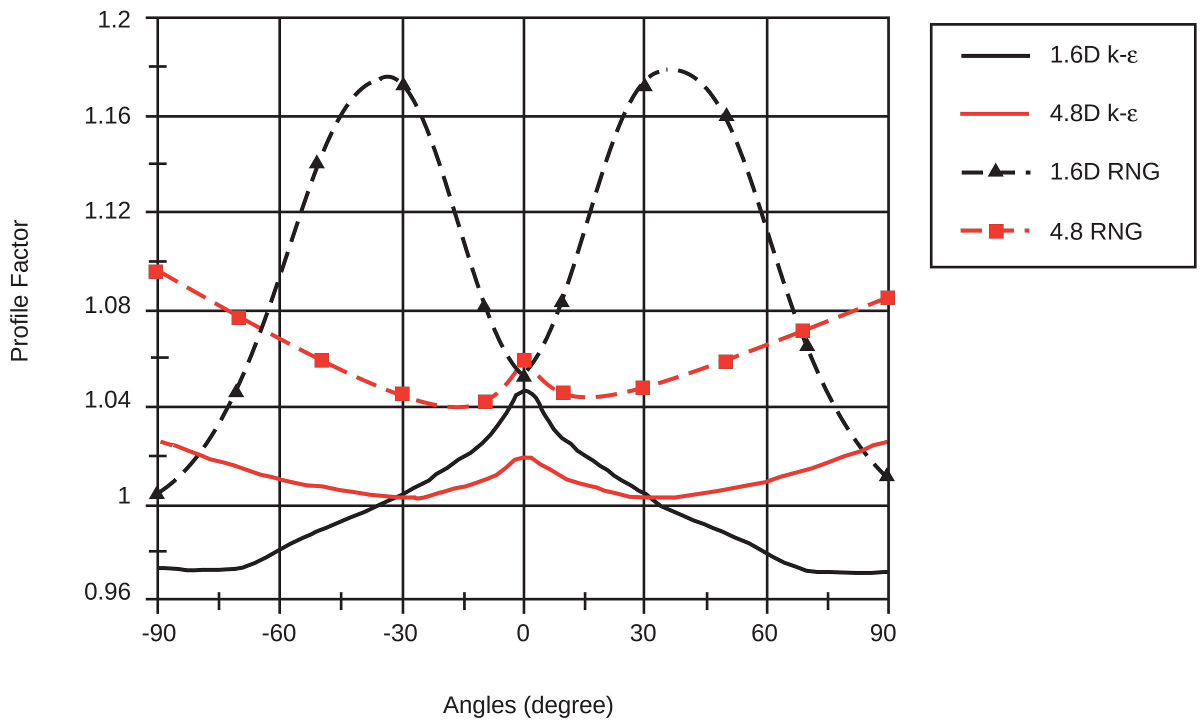

Figure B–5-5
Comparison of Profile Factors Calculated from Two Different Turbulence Models (Contraction Model)

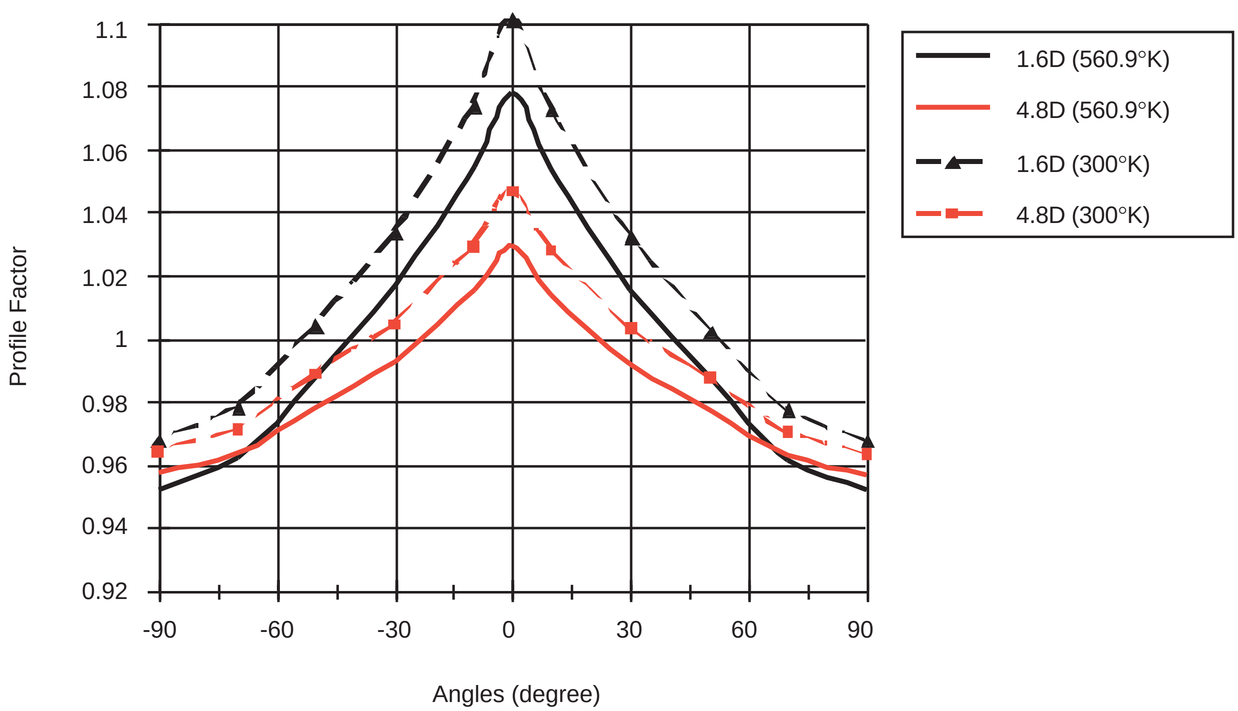

Figure B–5-6
Comparison of Profile Factors Calculated from Different Physical Properties of the Fluid: 560.9°K (549.95°F) at 1.55 x 10^7 Pa (2.25 x 10^3 psia) and 300.15°K (80.6°F) at 1.013 x 10^5 Pa (1.47 x 10^1 psia) (Spherical Head Model)

WARNING: This Document contains information classified under U.S. Export Control regulations as restricted from export outside the United States. You are under an obligation to ensure that you have a legal right to obtain access to this information and to ensure that you obtain an export license prior to any re-export of this information. Special restrictions apply to access by anyone that is not a United States citizen or a Permanent United States resident. For further information regarding your obligations, please see the information contained below in the section titled "Export Control Restrictions."

Export Control Restrictions
Access to and use of EPRI Intellectual Property is granted with the specific understanding and requirement that responsibility for ensuring full compliance with all applicable U.S. and foreign export laws and regulations is being undertaken by you and your company. This includes an obligation to ensure that any individual receiving access hereunder who is not a U.S. citizen or permanent U.S. resident is permitted access under applicable U.S. and foreign export laws and regulations. In the event you are uncertain whether you or your company may lawfully obtain access to this EPRI Intellectual Property, you acknowledge that it is your obligation to consult with your company's legal counsel to determine whether this access is lawful. Although EPRI may make available on a case by case basis an informal assessment of the applicable U.S. export classification for specific EPRI Intellectual Property, you and your company acknowledge that this assessment is solely for informational purposes and not for reliance purposes. You and your company acknowledge that it is still the obligation of you and your company to make your own assessment of the applicable U.S. export classification and ensure compliance accordingly. You and your company understand and acknowledge your obligations to make a prompt report to EPRI and the appropriate authorities regarding any access to or use of EPRI Intellectual Property hereunder that may be in violation of applicable U.S. or foreign export laws or regulations.

About EPRI

EPRI creates science and technology solutions for the global energy and energy services industry. U.S. electric utilities established the Electric Power Research Institute in 1973 as a nonprofit research consortium for the benefit of utility members, their customers, and society. Now known simply as EPRI, the company provides a wide range of innovative products and services to more than 1000 energy-related organizations in 40 countries. EPRI's multidisciplinary team of scientists and engineers draws on a worldwide network of technical and business expertise to help solve today's toughest energy and environmental problems.

EPRI. Electrify the World

Programs: TR-107327

Nuclear Power

Printed on recycled paper in the United States of America

EPRI • 3412 Hillview Avenue, Palo Alto, California 94304 • PO Box 10412, Palo Alto, California 94303 • USA
800.313.3774 • 650.855.2121 • askepri@epri.com • www.epri.com